



# **Integration of seismic interpretation in to geostatistical acoustic impedance**

**Sergio Cruz Bardera**

Thesis to obtain the Master of Science Degree in Petroleum Engineer

## **Master Degree in Petroleum Engineering**

Supervisor: Prof. Leonardo Azevedo Guerra Raposo Pereira

### **Jury**

President: Prof. Maria João Pereira Colunas Pereira  
Supervisor: Prof. Leonardo Azevedo Guerra Raposo Pereira  
Members of the Committee: Prof. Amílcar de Oliveira Soares

**November 2016**

## Resumo

Na modelagem de reservatório e caracterização diferentes técnicas de inversão sísmica são condicionados pelos dados existentes disponíveis fornecidas pelo estudo da sísmica e as propriedades petro-elástica de subsuperfície obtidas por poços, a solução do inversão tenta fornecer um modelo de subsuperfície que se encaixa de forma igual todos os dados observados existentes. Um quadro geoestatística é uma solução natural para integrar os dados dentro do mesmo quadro ao avaliar a incerteza espacial da propriedades invertidas. O objetivo principal desta tese é avaliar o desempenho de uma nova implementação dentro de uma metodologia de inversão sísmica geoestatística conhecida para recuperar modelos elásticos subsuperficiais (impedância acústica) para caracterizar um reservatório real, não-estacionária. A nova implementação do algoritmo de inversão sísmica geoestatística consiste em uma regionalização por zonas da área de estudo como forma de interpretar os dados existentes e o conhecimento sobre a geologia do subsolo. A metodologia proposta utiliza funções de distribuição multi-locais com base em algoritmos de simulação sequenciais diretos. O estudo de caso apresentado nesta tese consiste na inversão de um reais e complexos dados sísmicos partial-stacked onde três poços estão disponíveis. Os resultados obtidos pela metodologia proposta são comparados com os obtidos por um método convencional.

## **Abstract**

In reservoir modelling and characterization different seismic inversion techniques are conditioned by the available existing data provided by seismic surveys and the subsurface petro-elastic properties obtained by wells, the inversion solution tries to provide a subsurface model that fits equally all the existing observed data. A geostatistical framework is a natural solution to integrate both data within the same framework while assessing the spatial uncertainty of the inverted property. The main objective of this thesis is to assess the performance of a new implementation within a known geostatistical seismic inversion methodology to retrieve subsurface elastics models (acoustic impedance) to characterize a non-stationary real reservoir. The new implementation of geostatistical seismic inversion algorithm consists in a regionalization by zones of the study area as interpreted from the existing data and the knowledge about the subsurface geology. The proposed methodology uses multi-local distribution functions based on direct sequential simulation algorithms. The case study presented in this thesis consists in the inversion of a real and complex partial-stacked seismic data where three wells are available. The results obtained by the proposed methodology are compared with those obtained by a conventional approach.

**Key words:** Geostatistical seismic inversion; seismic reservoir characterization; geostatistics; direct sequential simulation; direct stochastic simulations; Global stochastic inversion.

## **Acknowledgements**

This work was created on the Center for Modeling Petroleum Reservoirs (CMRP) from CERENA, of Instituto Superior Técnico (IST), Universidade de Lisboa. I would like to thank to Professor Leonardo Azevedo to support me during all this year with this Project and trust me to do it.

I would also like to thank CERENA/CMRP, for supporting my thesis work and Partex Oil & Gas for providing me the necessary datasets to test and implement the new algorithms presented in this thesis, and thank Schlumberger for the academic donation of Petrel® license.

# Index

1	Introduction.....	1
1.1	Scope of the study .....	1
1.2	Objective and motivation .....	2
1.3	Overview of methodologies .....	2
1.4	Structure of the thesis.....	3
2	Methodology.....	5
2.1	Conventional Global Stochastic Inversion.....	5
2.2	Global Stochastic Inversion for non-stationary geological environments.....	7
3	Real case application .....	11
3.1	General overview of the background geology .....	11
3.2	Dataset description.....	14
3.3	Well logs .....	16
3.4	Division by zones.....	16
4	Geostatistical seismic inversion applied to the real case study .....	20
4.1	Conventional Global Stochastic Inversion.....	20
4.1.1	Inversion parametrization .....	20
4.1.2	Result.....	21
4.1	Global Stochastic Inversion for non-stationary geological environments.....	25
4.1.1	Inversion parametrization .....	25
4.1.2	Result.....	26
5	Discussion .....	30
6	Conclusion.....	34
7	References.....	35

## LIST OF FIGURES

<b>Figure 1-</b> Schematic representation of GSI (from Azevedo 2013) .....	6
<b>Figure 2-</b> Dataset obtained from each zone .....	7
<b>Figure 3 -</b> Dataset from well A1 by zones for AI property.....	8
<b>Figure 4 -</b> Examples of histograms by zones for one property, zone 0(left), zone 1(center), zone 2(right) .....	8
<b>Figure 5 -</b> Example of global cdf obtained from one zone with the conditional distribution centered by simple kriging and variance .....	9
<b>Figure 6 -</b> Generalized stratigraphic column of the basin (from USGS, Michael E. Brownfield and Ronald R. Charpentier).....	11
<b>Figure 7 -</b> Example of turbidity current and deposit sediments (from Wadsworth Publishing company 1998).....	13
<b>Figure 8 -</b> Schematic cross-section of the basin with the possible location of the study area (rounded in red) (from USGS, Michael E. Brownfield and Ronald R. Charpentier).....	14
<b>Figure 9 -</b> Cross section of the study case with the inversion area delimited by Partex and his location in the grid.....	15
<b>Figure 10 -</b> Comparison between the histograms of the original well-log data and the well-log data after the upscaling into the reservoir grid. From left of right: density, P-wave, S-wave velocities and density. The main statistics (mean and variance) are preserved after the upscaling process. ....	15
<b>Figure 11 -</b> well logs (A1, A3, A4) located along the study area preferentially drilling the geologic pay formation.....	16
<b>Figure 12 –</b> Cross-section of model definition that will be used in the proposed methodology with a regionalization by zones within the seismic grid.....	17
<b>Figure 13:</b> Top surface of the different zones (from 2 to8) with the contour lines every 100 meters ...	18
<b>Figure 14 -</b> Geometrical modeling in 3D created in Petrel program with a seismic resampling within the seismic grid to obtain the elastic properties by separation of zones with the location of the cross-section (red line) Figure 12.....	19
<b>Figure 15 -</b> Variograms, max(Left), min(center) and vertical(right). The variograms were computed using exclusively the set of conditioning well data. ....	20

<b>Figure 16</b> - Acoustic impedance values from wells, the intrinsic characteristic of the prior distribution estimated from the well log, mean variance and extreme values are preserved after the upscaling. ..	21
<b>Figure 17</b> - Comparison between vertical sections extracted from (on the left) acoustic model computed from the ensemble of models simulated during the last iteration and (on the right) synthetic seismic reflection data. From top to bottom: best AI model, mean AI model. For profile location see Figure 9.....	22
<b>Figure 18</b> - Global correlation coefficient between the recorded and the best inverted poststack seismic with a correlation of 0,951 (left) and between the recorded and the mean inverted seismic with a correlation of 0,946.....	23
<b>Figure 19</b> - Local correlation coefficient volume calculated on a trace by trace basis between the best-fit synthetic and the real seismic volume.....	24
<b>Figure 20</b> - Standard deviation that represents the distribution respect to the mean. ....	24
<b>Figure 21</b> - Histograms of Ip dataset of all zones 1 to 8.....	26
<b>Figure 22</b> - Comparison between vertical sections extracted from (on the left) acoustic model computed from the ensemble of models simulated during the last iteration and (on the right) synthetic seismic reflection data. From top to bottom: best AI model, mean AI model. For profile location see Figure 9.....	27
<b>Figure 23</b> - Global correlation coefficient between the recorded and the best inverted poststack seismic with a correlation of 0,91 (left) and between the recorded and the mean inverted seismic with a correlation of 0,89.....	28
<b>Figure 24</b> - Local correlation coefficient volume of the proposed methodology by zones calculated on a trace by trace basis between the best-fit synthetic and the real seismic volume.....	28
<b>Figure 25</b> - Standard deviation of the proposed methodology by zones that represent the distribution respect to the mean.....	29
<b>Figure 26</b> – Real seismic volume (on the top) and comparison between the results obtained for zone 1 in the traditional GSI with the best seismic model and standard deviation (left) and the results obtained with the methodology proposed by zones with the best seismic model and the standard deviation (right) .....	31
<b>Figure 27</b> - Real seismic volume (on the top) and more in detail (above right) and comparison between the results obtained for zone 4 in the traditional GSI with the best seismic model(left) and the results obtained with the methodology proposed by zones with the best seismic model(centre).....	32

**Figure 28** - Standard deviation of the traditional GSI result (left) and of the proposed methodology by zones (right) that represent the distribution respect to the mean..... 33



# 1 Introduction

The thesis was carried out under the Master of Petroleum Engineering in the Institute Superior Técnico, in particular CERENA - the Center for Natural Resources and Environment, with a real dataset provided by Partex Oil & Gas.

## 1.1 Scope of the study

Among the tools to identify potential hydrocarbon reservoir, 3D seismic volumes allow exploring a huge volume of area of the subsurface helping oil and gas companies to obtain enough information regarding the geological structures and predict the best locations to drill wells. Depending on the existing data, there are different ways to build 3D models and different modeling techniques allow obtaining models with variable degrees of detail. However, independently of the methodology, all of them have some degree of uncertainty. Choosing the right modelling approach allow decreasing the risk level and consequently the costs related with a given hydrocarbon reservoir, and consequently allowing better management decisions (Doyen 2007; Caers 2011).

In order to achieve more reliable 3D models the companies use seismic reflection data to estimate the subsurface geology properties and fluid distribution, instead of the traditional seismic interpretation approach where seismic reflection data is exclusively used for constraining the reservoir's geometry (Bosch et al 2010).

In petroleum applications, stochastic modeling of the reservoirs' internal properties, such as lithofacies and sand bodies, is normally done by using core and log data which locally provide detailed reservoir information but lack spatial information, therefore, these models have great level of uncertainty far from the wells locations. For this reason the integration of seismic reflection data, take into account the properties directly measured at the wells, allow inferring more reliable subsurface models with less uncertainty, i.e., better spatially constrained.

Normally seismic inversion methodologies take into account stacked seismic reflection data allowing the inference of acoustic and/or impedance models. Inferring the spatial distribution of impedance limits the identification of different litho-fluid facies of interest that could be obtained using pre-stack seismic data. The proliferation of high quality pre-stack seismic data allows us to obtain more reliable, with less uncertainty, reservoir models when compared with reservoir models derived exclusively from post-stack seismic reflection data.

Iterative geostatistical seismic inversion methodologies are a common modelling technique in Earth science allowing the simultaneous integration of well-log and seismic reflection data. These seismic inversion methodologies use stochastic sequential simulation as the model perturbation technique. Traditional stochastic sequential simulation techniques assume for the entire study area stationarity of

the spatial continuity pattern and a single probability distribution function as inferred from the available experimental data respectively. This problem can be tackled by using multi-local distribution functions taking into consideration a multiple regionalization by zones (Azevedo, 2013).

The work presented in the next chapters of this thesis tries to give new insights for the geostatistical seismic reservoir characterization within methodologies already known. This work has a particular focus on a novel geostatistical seismic inversion methodology that is able to deal with non-stationary geological environments

## 1.2 Objective and motivation

The main objective of this thesis is the implementation on a real and challenging dataset of a new geostatistical seismic inversion that is able to deal with non-stationary geological environments. The results obtained are compared against those retrieved from conventional iterative geostatistical seismic inversion methodology.

This Master thesis provides a novel approach within geostatistical methodologies already known for stochastic post-stack seismic inversion. The proposed workflows allow for more reliable reservoir models by allowing the assessment of the spatial uncertainty related with the properties of interest. The main objectives of this work may be summarized by the following:

- Implementation of the conventional global stochastic inversion GSI (Soares 2007) that uses a global approach during the stochastic simulation stage and allows the inversion of fullstack seismic reflection data for acoustic impedance (AI) models.
- Development and implementation within the GSI framework of a new methodology to handle multi-local distribution functions and spatial continuity patterns taking into consideration a regionalization of the study area by zones.

The development of these algorithms was performed recurring to geostatistical toolboxes from CERENA/CMRP research group and Matlab. Petrel® (Schlumberger) was used for visualization of the results.

## 1.3 Overview of methodologies

Nowadays to obtain reservoir models as close as possible to reality we use inverted acoustic model inferred from existing seismic reflection data and integrating information from existing wells. However, in order to derive petro-elastic properties from seismic reflection data we need to solve an inverse problem. Seismic inversion problem is characterized for being nonlinear, with non-unique solution and ill-conditioned. Due to this reason the inverted acoustic models are only one possibility among several models that equally satisfy the observed seismic reflection data. Regardless of the method chosen to solve the seismic inverse problem, there is always the uncertainty associated with the acoustic model,

so here is important to ensure that the uncertainty is assessed continuously and spreads throughout the investment process.

Seismic inversion solutions can be divided in two main approaches: deterministic, and probabilistic (Bosch, Mukerji, and González 2010).

- Deterministic methods are generally based on minimizing the differences between synthetic and observed seismic reflection data, based on the convolutional model and only allow inferring a single best-fit inverse model (Francis, 2006).

- In the probabilistic setting there are two main approaches to solve the seismic inversion problem: the Bayesian linearized framework and the one based on stochastic sequential simulation as the model perturbation technique.

Bayesian approaches ensure the propagation of the uncertainty from the prior probability distributions, estimated from experimental data (e.g. well-log data) to the probability distributions of the model parameters space (Grana et al. 2012). This framework assumes a linearized forward model and Gaussian, or multi-Gaussian, for the prior distribution function of the property to be inverted. In this setting the posterior distribution can be analytically expressed as multi-Gaussian.

Alternatively stochastic inversion methodologies allow a more comprehensive exploration of the model parameter space because the assumption about any prior parametric probability distribution may be relaxed depending on the stochastic sequential algorithm used within the inversion procedure. Traditional stochastic sequential simulation technique assume for the entire study area stationary of the spatial continuity pattern and a single probability distribution function, as revealed by a single variogram model as inferred from the available experimental data. In this thesis we extended the traditional direct sequential simulation algorithm to handled non-stationary natural phenomena take into consideration multiple regionalized spatial continuity patterns a probability distribution functions depending of the spatial location of the grid node to be simulated.

## 1.4 Structure of the thesis

This thesis is divided in fives Sections:

The present section (section 1) comprises the introduction divided in different sections: objective and motivation that led to the research of this thesis, a scope of the study where is identified and describe the problem and a briefly overview of the main methodology used.

Section 2 introduces a broad description of the methodology used already knows and the novel proposed methodology applied to the methods described above.

Section 3 present the study area with a geological brief introduction, showing the different physical properties used for a real case with dataset provided by Partex Oil & Gas, well logs and a description and explication the regionalization of the study area.

In Section 4 the algorithms introduced in the previous chapter were tested and implemented in the case study and shown the result of applying the proposed methodology by zones as a part of the geostatistical seismic inversion methodology.

In the last section (Section 5) presents a brief discussion and conclusion comparing the final results obtained in the previous chapter with the traditional approach GSI.

## 2 Methodology

### 2.1 Conventional Global Stochastic Inversion

The methodology used as the basis to develop the new methodology proposed under the scope of this thesis was the Global Stochastic Inversion (GSI, Soares 2007). The traditional GSI procedure uses a stochastic sequential simulation algorithm based on a single distribution function as estimated from the available well-log data and a single spatial continuity pattern as expressed by a variogram model for the entire study area. This methodology uses a global approach during the stochastic simulation stage and allows the inversion of fullstack seismic data for acoustic impedance (AI).

This iterative geostatistical methodology is based on two key main ideas: the use, at the end of each iteration, of a global optimizer based on cross-over genetic algorithm based on the trace-by-trace match between synthetic and the seismic data to ensure the convergence of the inversion procedure from iteration to iteration; and the perturbation of the inverted models with stochastic sequential simulation, the direct sequential simulation (DSS; Soares et al 2007).

This methodology generates for an entire seismic grid a set of  $N_s$  impedance models using existing well-log data as experimental data. Each impedance model is then convolved for the wavelet to create  $N_s$  synthetic seismic volumes which are compared on a trace-by-trace basis against the observed seismic reflection data. With this approach the areas of low signal-to-noise ratio remain poorly matched at the end of the inversion process. Contrary to the trace-by-trace approaches, an ensemble of best-fit inverted models will always present high uncertainty, for those noisy areas where the signal-to-noise ratio is low (Figure 1).

The GSI may be summarized in the following sequence of steps:

- First, a set of  $N_s$  acoustic impedance models, conditioned to the available acoustic impedance well-log data, is performed using DSS. Each realization of acoustic impedance reproduces the well-log data at its locations and the global distribution as inferred from the available experimental data and a single spatial continuity pattern as revealed by a variogram model;
- Then, from this set of impedance models a corresponding set of  $N_s$  synthetic seismic volumes is derived by computing the corresponding normal incidence reflection coefficients (1) which are then convolved by an estimated wavelet for that particular seismic dataset;

$$RC = \frac{AI_2 - AI_1}{AI_2 + AI_1}$$

(1)

Where the indexes 1 and 2 correspond, respectively, to the mean above and below the reflection interface considered;

- Each seismic trace from the  $N_s$  synthetic seismic volumes is then compared in terms of correlation coefficient against the real seismic trace from the same location;
- From the ensemble of simulated AI models, the acoustic impedance traces that produce synthetic seismic that ensure the highest correlation coefficient when compared with the corresponding real seismic trace are stored. These stored volumes, the one with the best acoustic impedance traces and the one with the local correlation coefficients, are used as secondary variables, or seeds, for the generation of the new set of acoustic impedance models for the next iteration.
- The iterative procedure finishes when the global correlation coefficient between the synthetic and the real seismic volumes is above a certain threshold (Soares et al. 2007).

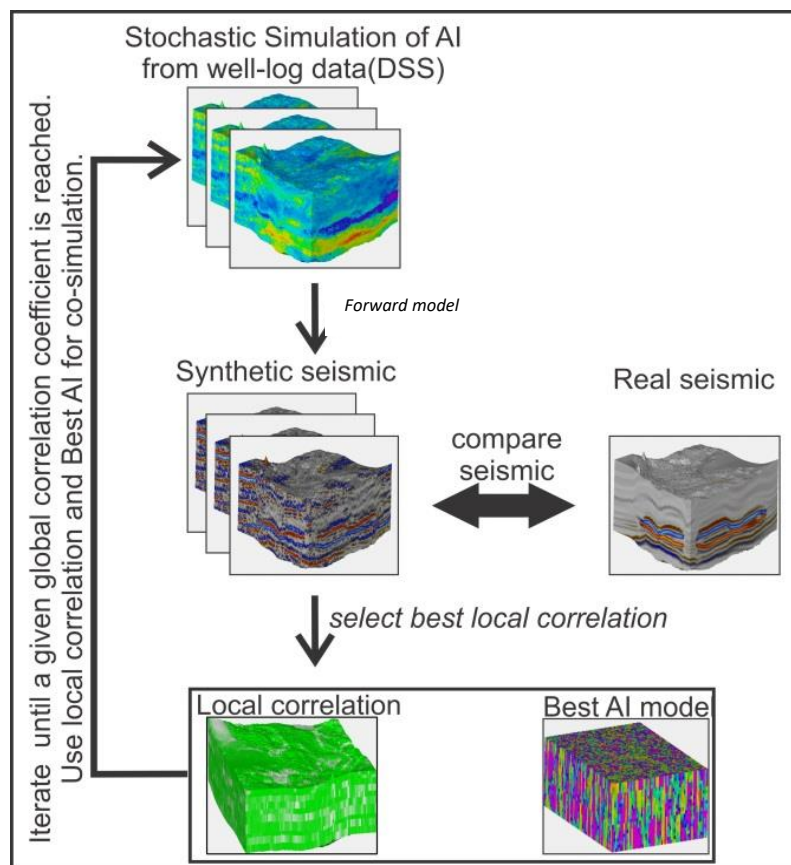


**Figure 1-** Schematic representation of GSI (from Azevedo 2013)

## 2.2 Global Stochastic Inversion for non-stationary geological environments

This section introduces the proposed geostatistical seismic inversion methodology that is able to simultaneously integrate a regionalization model based in zones. The regionalization model may be created based on the simultaneous interpretation of seismic and well-log data and geological constrains from a priori knowledge of the geology. Each zone will be constrained by a given distribution function and his corresponding spatial continuity patterns as inferred from the experimental data (the available well-log given for each zone and a variogram model by zone).

The definition of the regions within the inversion grid does not need to be regular as the proposed methodology is able to deal with regions with considerable different shapes and size.

In the proposed methodology the inversion area is first subdivided in zones. This zonation of the study area may be arbitrary, based on a priori knowledge of the natural system one is modelling or taken from seismic facies interpreted from available seismic reflection data. The number of regions its individual size and shape are defined deterministically. It is important to highlight that a division of the area in too many zones do not ensure a good inversion, i.e., each zone must be statistically representative. The number of zones from which the methodology is unreliable is out of the scope of this thesis.

The methodology can be summarized in the following sequence of steps (Azevedo et al. 2016):

- The first step comprises the generation of a geological model as realistic as possible and the division of the entire study area into smaller zones which should be geologically consistent. The independent simulation of each region is not feasible since it does not ensure the reproduction of the global statistics as inferred from the global available experimental data. Also, this approach may result in discontinuities at the boundaries of each sub-region.

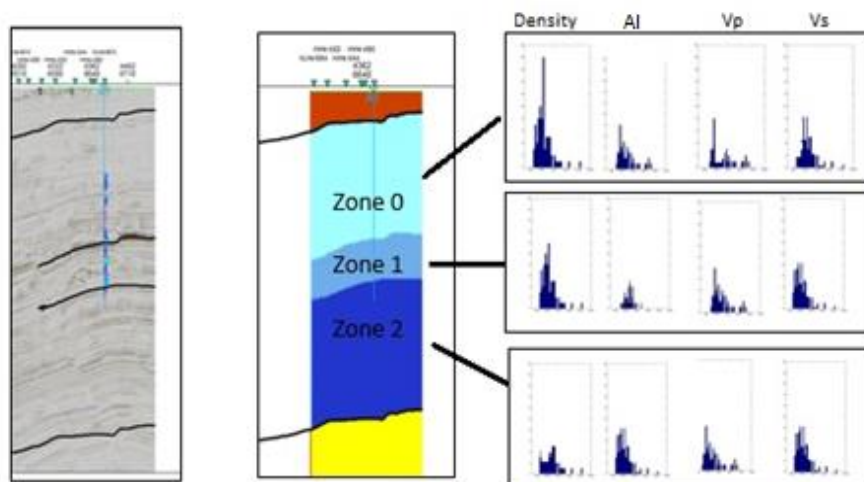


**Figure 2-** Dataset obtained from each zone

- For each zone a histogram (one for each elastic property of interest such as density,  $V_p$ ,  $V_s$  or AI) is assigned for each zone, the spatial continuity pattern of the property to be simulated is conditioned by the imposed variogram model for each zone individually.
- Taking into account the regionalization model, the available dataset is extracted from wells as a function of the zones thus obtaining each model for each zone (Figure 3 and Figure 4).

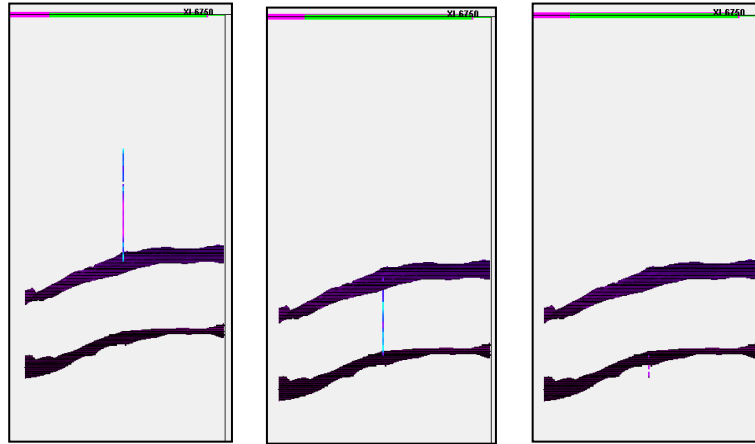


**Figure 3** - Dataset from well A1 by zones for AI property

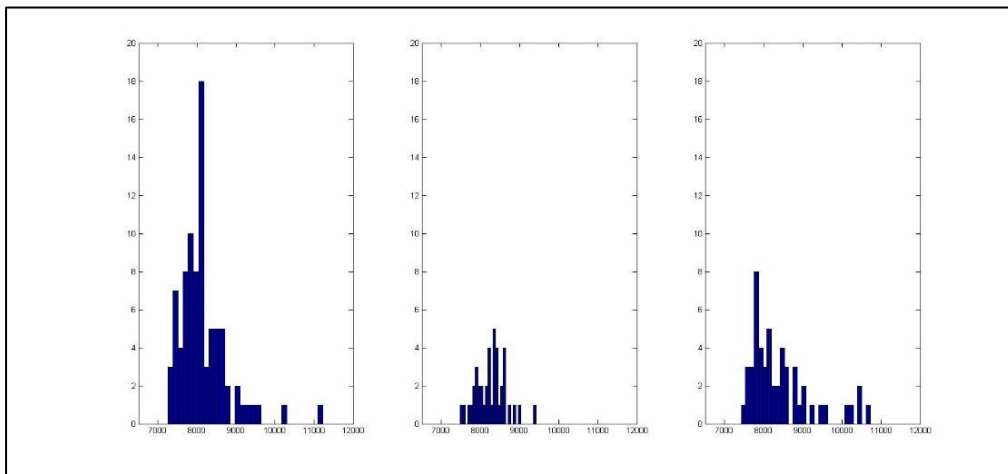


**Figure 4** - Examples of histograms by zones for one property, zone 0(left), zone 1(center), zone 2(right)

- Generated of a random seed to define a random path over the entire simulation grid,  $u = 1, \dots, N$ , where  $N$  is the total number of nodes that compose the simulation grid and “ $u$ ” is the current node location where the simulation is being performed.
- Estimation of the local mean and variance at  $x_u$  with simple kriging estimate  $[Z(x_u)^*]$  (2) and the corresponding kriging variance  $(\sigma^2(x_u))$  (3) to sample directly from the global conditional distribution function as estimated from the experimental data  $(z(x_\alpha))$  located within a specific zone and the previously simulated data  $(z(x_\alpha)^*)$  within a neighbourhood around  $u$ .



$$\frac{1}{n} \sum_{i=1}^n z(x_i) = [z(x_u)]^* \quad (2)$$

$$\frac{1}{n} \sum_{i=1}^n [z(x_i) - [z(x_u)]^*]^2 = \sigma_{sk}^2(x_u) \quad (3)$$

These global conditional distribution functions are going to be conditioned by the zones, however it is important nothing that, the simple kriging estimate and variance are computed taking into account point data that belong to different regions. The simple kriging estimate and variance are computed with all the point data within a given neighbourhood that may cross different sub-regions. This is an important feature of the proposed approach since it avoids the generation of discontinuities at the boundaries of each region in the simulated models.

- Definition the interval of the  $F_z(z)$  (conditional distribution) to be sampled based on the simple kriging estimate and variance computed from the previous step (Figure 5).  $F_z(z)$  corresponds to the probability distribution function of the variable to be simulated and estimated from the available experimental data that is located within that specific zone.

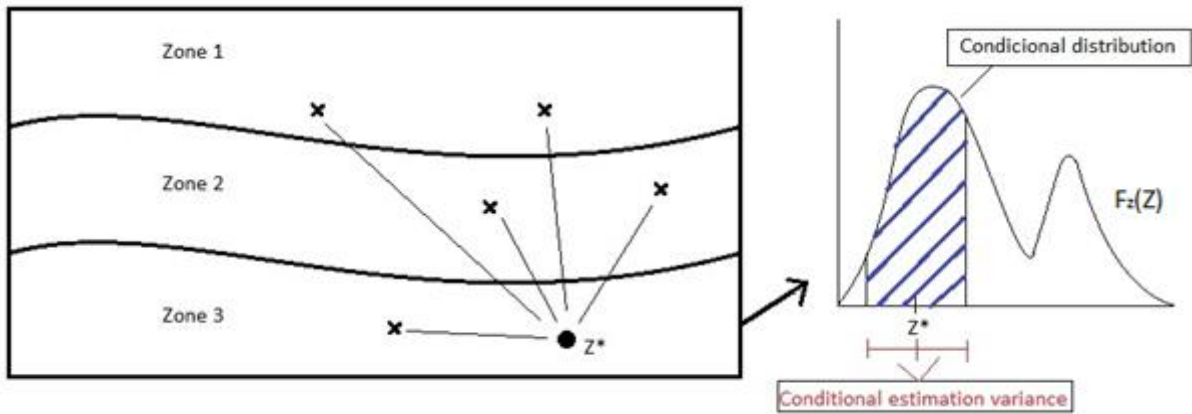


**Figure 5** - Example of global cdf obtained from one zone with the conditional distribution *centered* by simple kriging and variance

- The simulated values  $z^s(x_0)$  are drawn from an auxiliary Gaussian probability distribution function  $F_z'(z)$  which is built from the global cdf  $F_z(z)$ ,  $F_z'(z)$  is defined by selecting an interval over  $F_z(z)$  centered on the simple kriging estimate  $[Z(x_u)]^*$  value with an interval range proportional to the kriging variance ( $\sigma^2(x_u)$ ). Generate a value  $y^s$  from a Gaussian distribution  $((x_0)^*, \sigma^2_{sk}(x_u))$ . Return the simulated value  $z^s(x_0) = \varphi^{-1}(y^s)$
- Add the simulated value as conditioning for the simulation of the next location.
- Loop until all the  $N$  nodes of the simulated grid have been simulated.

The models resulting from the proposed stochastic sequential simulation reproduce simultaneously the regional and global variogram models and target distribution functions relative to the average volume of each zone (Azevedo et al. 2016).

In term of inverse procedure this work proposes replacing the traditional stochastic sequential simulation in the methodology summarized in (Figure 1) with the stochastic sequential simulation with multi-local distributions. The proposed iterative inversion methodology may be summarized such as:

- stochastic sequential simulation of Ns AI models simulated with DSS taking into account the regionalization model;
- synthetic seismic data calculation from the Ns Ip models previously simulated;
- comparison on a trace-by-trace basis against the observed seismic data;
- Selection of the best local correlation coefficient of a given iteration along with the elastic traces;
- Use the best local correlation coefficient volume and the corresponding Ip traces as secondary variable for the co-simulation of a new ensemble of Ip models;
- The iterative procedure stops when the global correlation coefficient is above a certain threshold. At the end the retrieved inverse models should be more geologically realistic, since they incorporate the knowledge of the subsurface geology.

### 3 Real case application

#### 3.1 General overview of the background geology

The available real dataset, where the methodology described in the previous chapter was implemented, is located in an area characterized as a huge salt basin that has undergone a complex geological history and can be divided into stages of basin development: pre-rift stage (late Proterozoic to Late Jurassic), syn-rift stage (Late Jurassic to Early Cretaceous), and post-rift stage (Late Cretaceous to Holocene) (Figure 6).

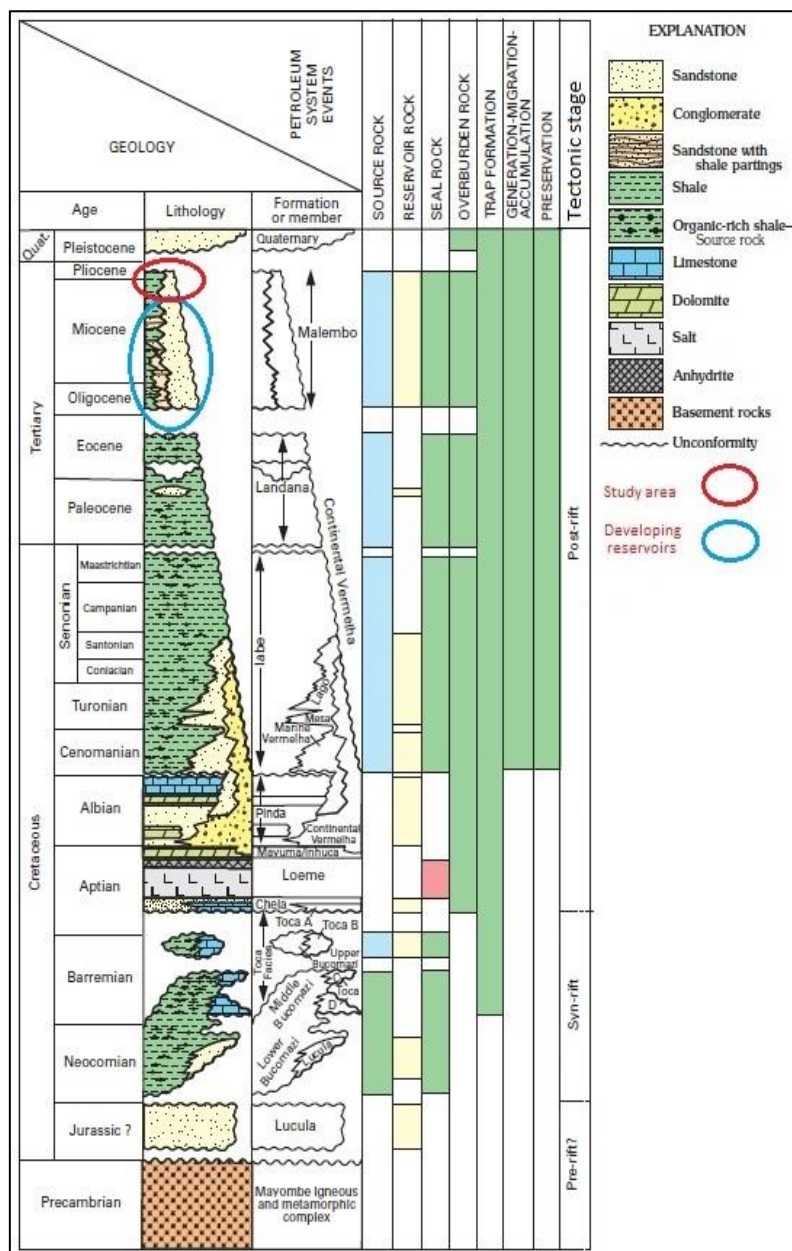


Figure 6 - Generalized stratigraphic column of the basin (from USGS, Michael E. Brownfield and Ronald R. Charpentier)

This sedimentary basin can be divided into a number of sub-basins aligned in a north-south direction and delimited by an east-west-trending fault system and other structural arches and highs related to syn-rift tectonics (Brownfield and Charpentier 2006).

Pre rift stage:

The pre-rift stage lasted through the Late Jurassic and incorporated several phases of intracratonic faulting and downwarping during which as much as 600 m of continental clastic rocks of Carboniferous to Jurassic age were deposited in the Interior subbasin.

Pre-rift rocks in this basin are limited to the Jurassic Sandstone, which directly overlies Precambrian basement. This unit consists of well-sorted, quartzes, micaceous sandstone and was most likely deposited as alluvial or eolian sands. The total thickness of pre-rift rocks in the Basin is unknown, but more than 1,000 m of clastic rocks have been penetrated in some wells.

Syn rift stage:

Initial rifting in the salt basin formed a series of asymmetrical horst-and-graben basins trending parallel to the present-day coastline. Thick sequences of fluvial and lacustrine rocks were deposited in the rift basins forming turbidities deposits. Organic-rich, lacustrine rocks of the rift stage are some of the most important hydrocarbon source rocks in these basins.

Post rift stage:

Post-rift rocks from Aptian to Holocene in age represent the initial opening of the Atlantic Ocean. The initial post-rift rocks are of early to mid-Aptian age and consist of continental, fluvial, and lagoonal rocks that were deposited as rifting ceased in the province. A period of extensive deposition of evaporates units, mainly salt, followed. Younger post-rift rocks were generally deposited in two distinct regimes: as transgressive units and as open-ocean deep-water units.

The area of interest basin covers 115,000 square km from shoreline to water depths of 3500 meters. In this basin has been discovered a lot of potential reservoir from tertiary age this led to focus in the deep-water turbidities sand associated with a large river within the continent.

The turbidities systems located in different sedimentary basins around the world actually have a high economic interest, while more than 80% of the giant oil fields in production developed in this type of sedimentary systems. Thus, understanding how they are formed and their characteristics is vital for oil exploration, so the turbidic channels and other associated elements as overflow deposits are currently the target of oil studies. (USGS, Michael E. Brownfield and Ronald R. Charpentier)

Turbidities are not characteristic of a particular tectonic environment, turbidite sequence is the result of the transport and deposition of sediments due to turbidity current deep-water any tectonic condition. (Figure 7).

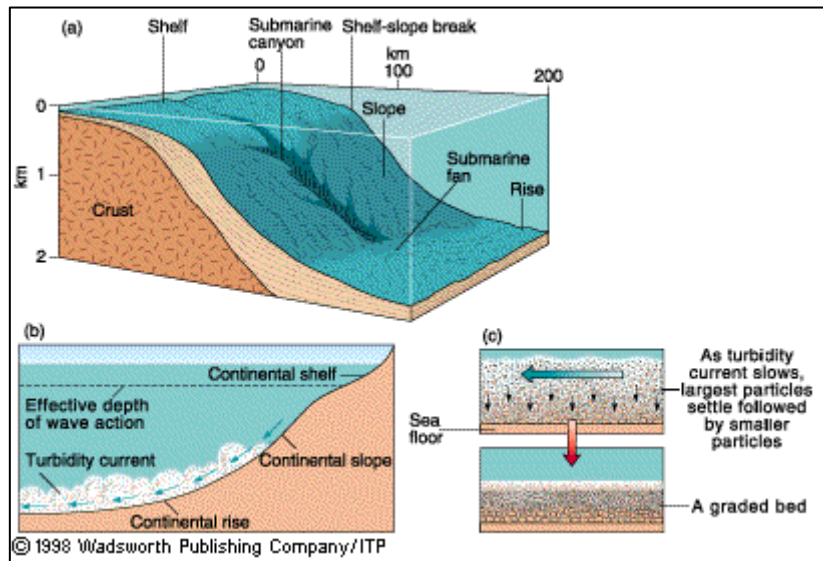


**Figure 7** - Example of turbidity current and deposit sediments (from Wadsworth Publishing company 1998)

The oil and gas production is intimately related to its working petroleum systems, which are primarily Lower Cretaceous and Tertiary in age. The geological evolution began during the Early Cretaceous with the continental break-up of Gondwana. Lacustrine rift basins developed in extensive north-south trending linear. The now-famous major source rock, an organically rich lacustrine shale known as the Bucomazi Formation (Figure 6) fed oil into the recently-formed Kwanza Basin pre-salt traps as well as into the numerous Pinda carbonate oil fields in the basin.

The primary source rock for the Delta Composite Total Petroleum System is the syn-rift Lower Cretaceous lacustrine shales of the Bucomazi Formation. Additional marine source rocks from the post-rift section are marine shales and marls of the Upper Cretaceous Labe Formation, the Paleocene to Eocene Landana Formation, and the Oligocene to Miocene Malembo Formation.

Oil generation began in the Late Cretaceous and has continued to the present. The migration pathways are mostly fault related, but some lateral migration has occurred below the Loeme Salt within the Chela Sandstone. Lacustrine oils charged many of the Upper Cretaceous and Tertiary turbidite channels and sandstones in the Basin (Schoellkopf and Patterson, 2000).

In the shallow-water areas, of the Basin, the majority of reservoir rocks are sandstones of both syn-rift and post-rift age, traps are mostly anticlinal. Some are relate to rollovers. Other traps are related to fault blocks or paleotopography. Seals are Cretaceous to Tertiary lacustrine and marine shales. In deeper water, reservoir rocks are expected to represent primarily Oligocene and Miocene turbidities

channels and basin-floor fans and mounds, traps are both stratigraphic and structural and include turbidite channels and sandstones, growth-fault-related sandstones sealed by shales.

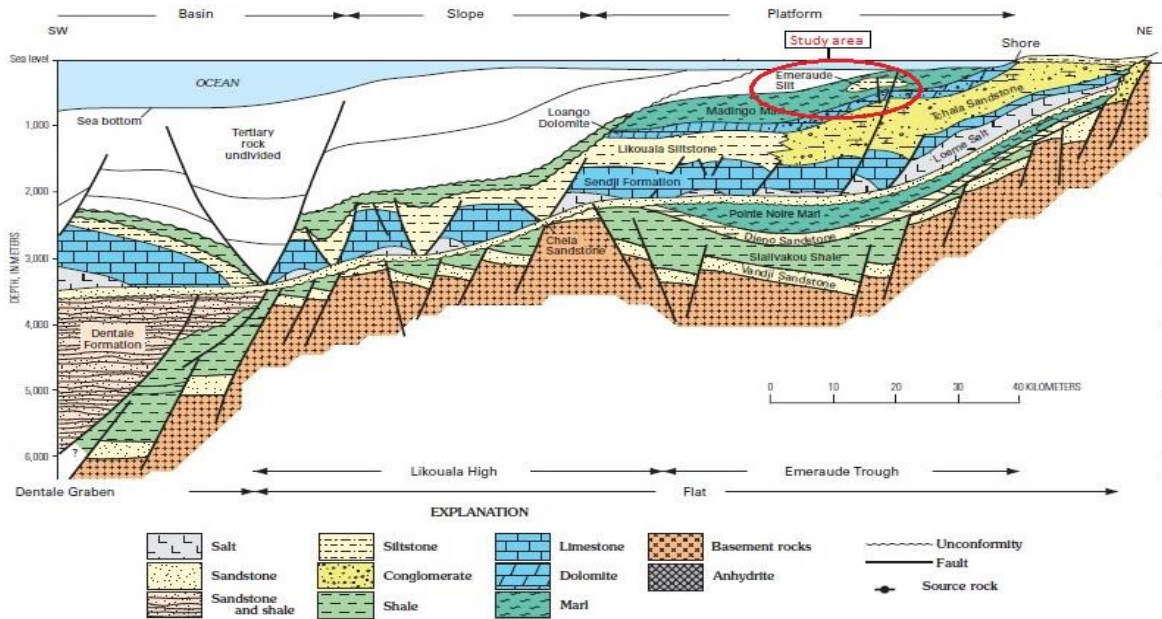


**Figure 8** - Schematic cross-section of the basin with the possible location of the study area (rounded in red) (from USGS, Michael E. Brownfield and Ronald R. Charpentier)

### 3.2 Dataset description

The study area is located within an offshore turbidite environment in a medium-to-deep water environment with a large turbid channel that runs the entire study area in north-east to south-west direction. The known reservoirs are easily recognized on partial angles stack due to amplitude anomalies with the offset.

The available data set comprised partial seismic volumes of 794 inline by 1194 crossline with a sampling rate of 4 ms. From the entire study area an inversion grid was defined such as 398 x 598 x 200 and vertically delimited by within the interval of interest from 1100 ms to 1700 ms (Figure 9) inversion area delimited by Partex. A set of 3 wells with  $V_p$ ,  $V_s$  and density logs was also available. Notice a few P-wave velocity data in the well 4 located within the inversion area and that subsequently, this lack of information will have repercussions on the final model, however all data from wells 1 and 3 are located within the inversion area. A wavelet extracted from each partial angle stack individually was also made available.

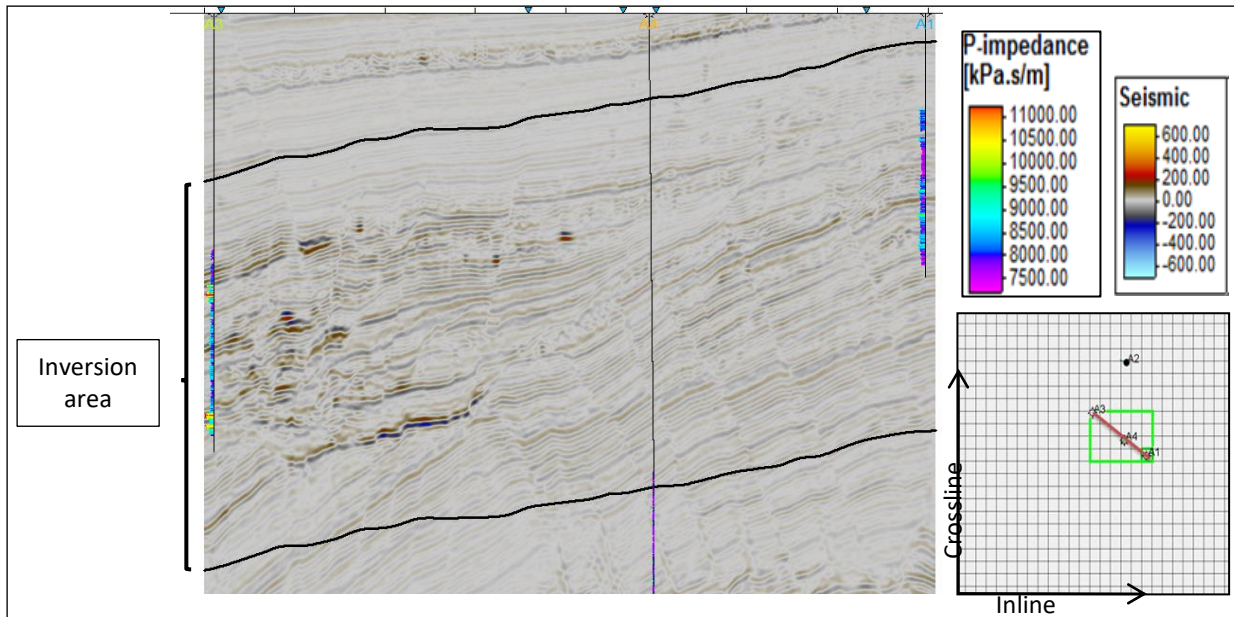


**Figure 9** - Cross section of the study case with the inversion area delimited by Partex and his location in the grid.

The wells are located along the study area preferentially drilling the geologic pay formation. These wells were previously tied to the available seismic reflection data and the resulting angle-dependent wavelets were also available. Any question related to the seismic to well tie and wavelet extraction procedures are out of the scope of this thesis. The high-resolution well-log data were upscaled into the reservoir grid ensuring that the extreme values, the mean and variance as retrieved from the original well-log data were preserved after the upscaling.

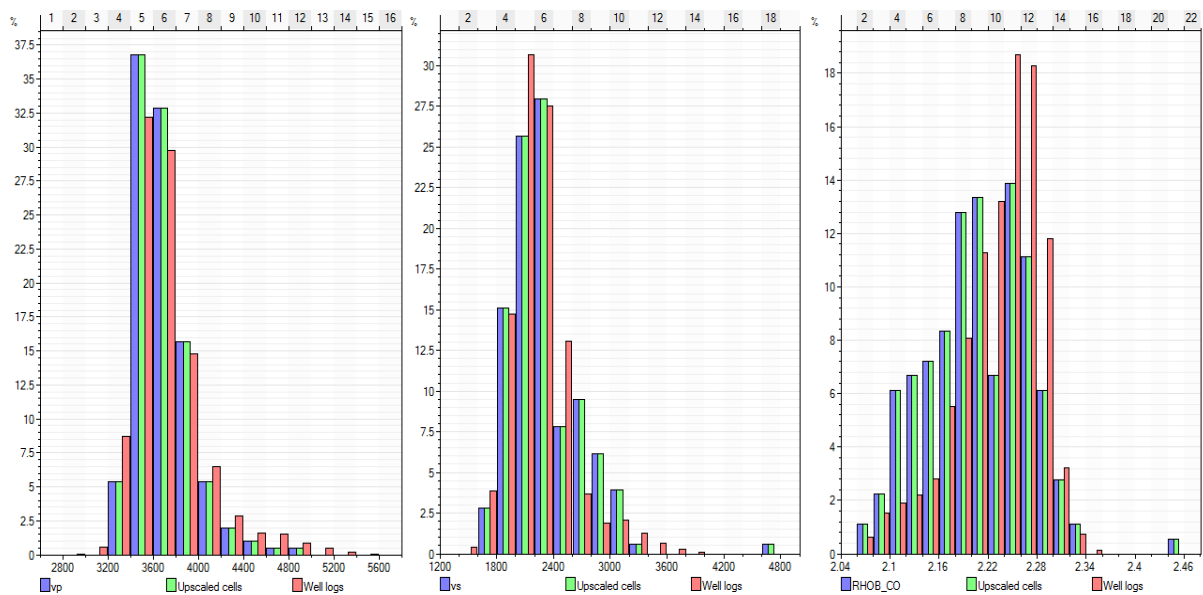


**Figure 10** - Comparison between the histograms of the original well-log data and the well-log data after the upscaling into the reservoir grid. From left of right: density, P-wave, S-wave velocities and density. The main statistics (mean and variance) are preserved after the upscaling process.

### 3.3 Well logs

The inversion grid encompasses the three well (A1, A3, A4) preferentially drilling the geologic pay formation. The well-log data (Figure 11) was used along with the seismic reflection data to define different zones within the inversion grid. The Figure below show the bottom of the zones considered to generate the regionalization model.

The proposed methodology is conditioned by the location of the existing experimental data, i.e., the wells locations. Figure 11 shows that the experimental data is mainly located between zones 2 and 5. The lack of data within all the zones represents a challenge for this application example.

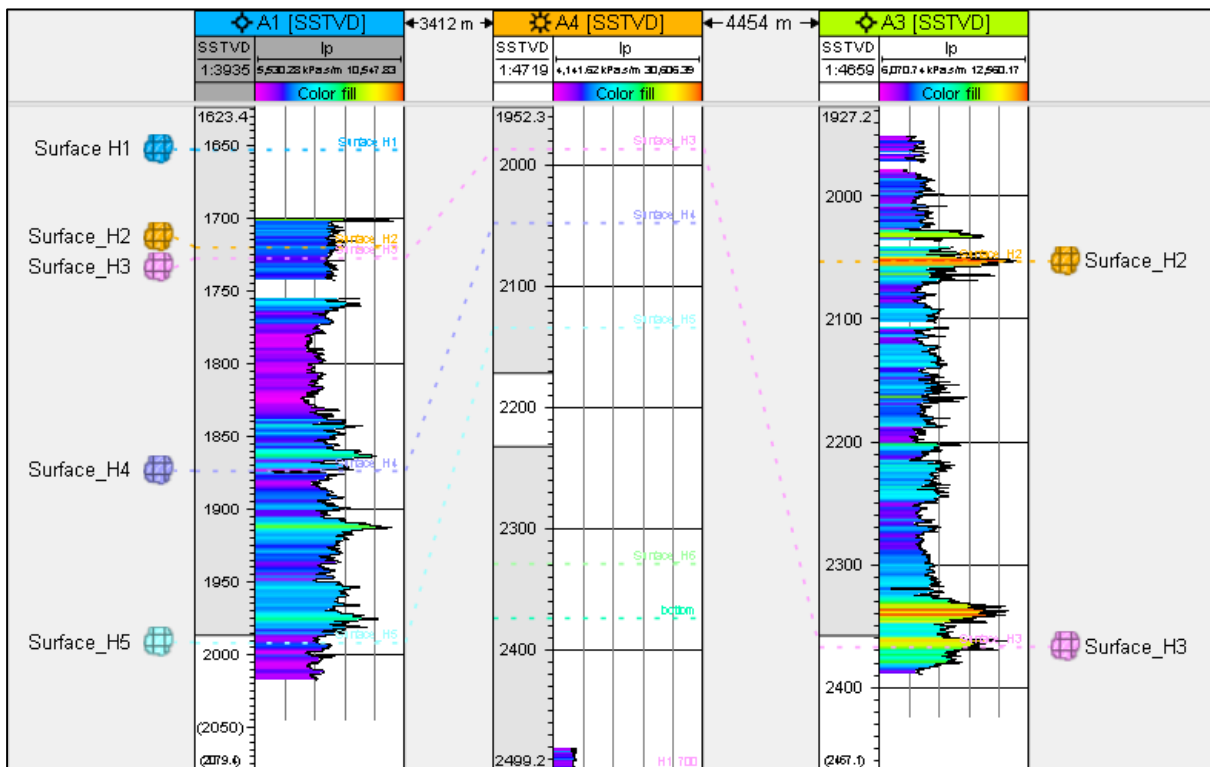


**Figure 11** - well logs (A1, A3, A4) located along the study area preferentially drilling the geologic pay formation.

### 3.4 Division by zones

The study area is located in a high-energy turbiditic depositional environment that is expressed in term of rapid variations of the amplitudes content of the recorded seismic reflection data. The simultaneous interpretation of the available properties logs for the different wells along with the seismic reflection data was used to divide the study area in eight vertical zones as showed in Figure 12 (division by zones), Figure 13 (interpreted horizons) and Figure 14 (geometrical modelling in 3D created in Petrel program). But this regionalization depends on the study area, the amount of information from the wells, the target and the interpretation of the geologist that the methodology applies.



Vertically in figure 13 the upper surfaces of the different zones can be observed with a clear east-west direction, and delimited by a west-east trending fault system very complex, that makes it difficult to interpret the seismic reflection data and other structural arches. The real seismic reflection data is highly non-stationary where different seismic units can be easily interpreted. In principle, the interpretation of the zones began taking into account the cross-section (Figure 12) that included the 3 wells and therefore the information necessary to carry out the simulations.

From here due to the complexity to interpret all the channels individually, it was decided to interpret the base and top of the main turbiditic channel (corresponding to zone 3). This zone comprises small channels related with different temporal episodes with not continuous values of seismic reflection data and without a clear delimitation. For the rest of the zones it is clear a simple vertical grid division based on surfaces parallel to top and zone 1, in this case the bottom of the inversion grid is not enough to properly describe the geological complexity of the study area.

Each zone considered for the generation of the regionalization model does not match perfectly the top and base of each seismic unit as inferred from traditional seismic interpretation procedure. This decision it is important and allows including the non-stationary behaviour as interpreted from the well-log data.

The geological interpretation has to be as realistic as possible, since each zone will have the same properties in depth and therefore the same probability distribution function, it is important to highlight that a high number of zones do not ensure a good inversion. Note that each zone should be statistically significant in order to invert for reliable acoustic models. If a zone is too small or thin, there will be a lack of experimental data to infer the corresponding distribution and spatial continuity pattern.

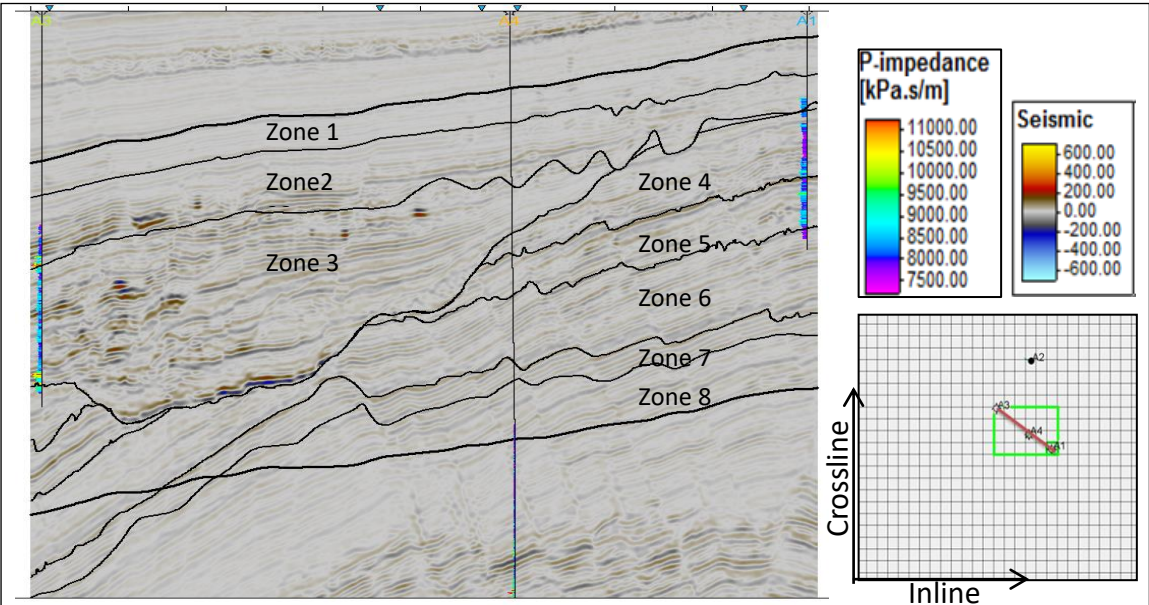


**Figure 12** – Cross-section of model definition that will be used in the proposed methodology with a regionalization by zones within the seismic grid.

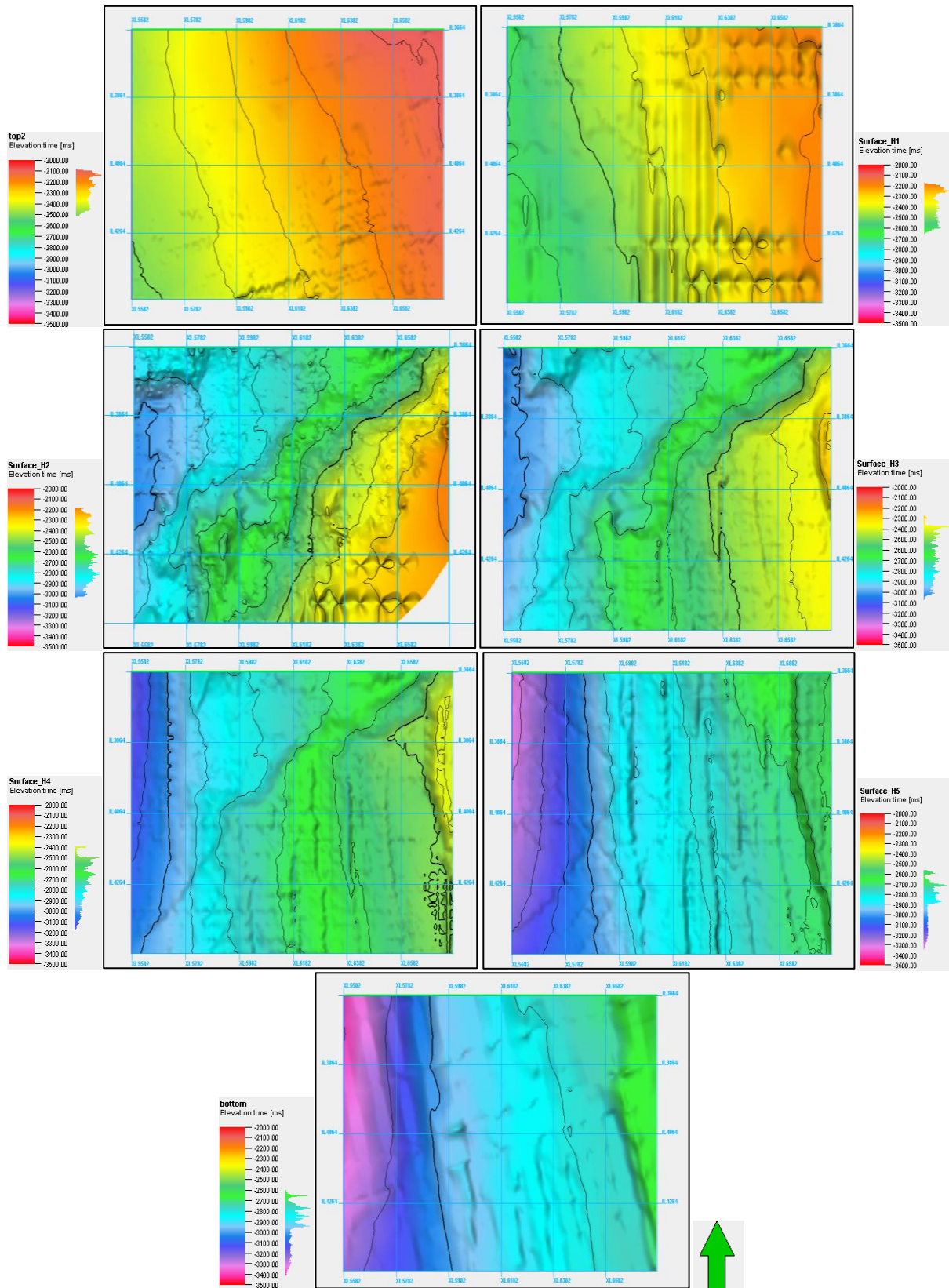


**Figure 13:** Interpreted horizons that represent top surface of the different zones from 2 to 8 (From top to bottom) with the contour lines every 100 meters and the range of values.

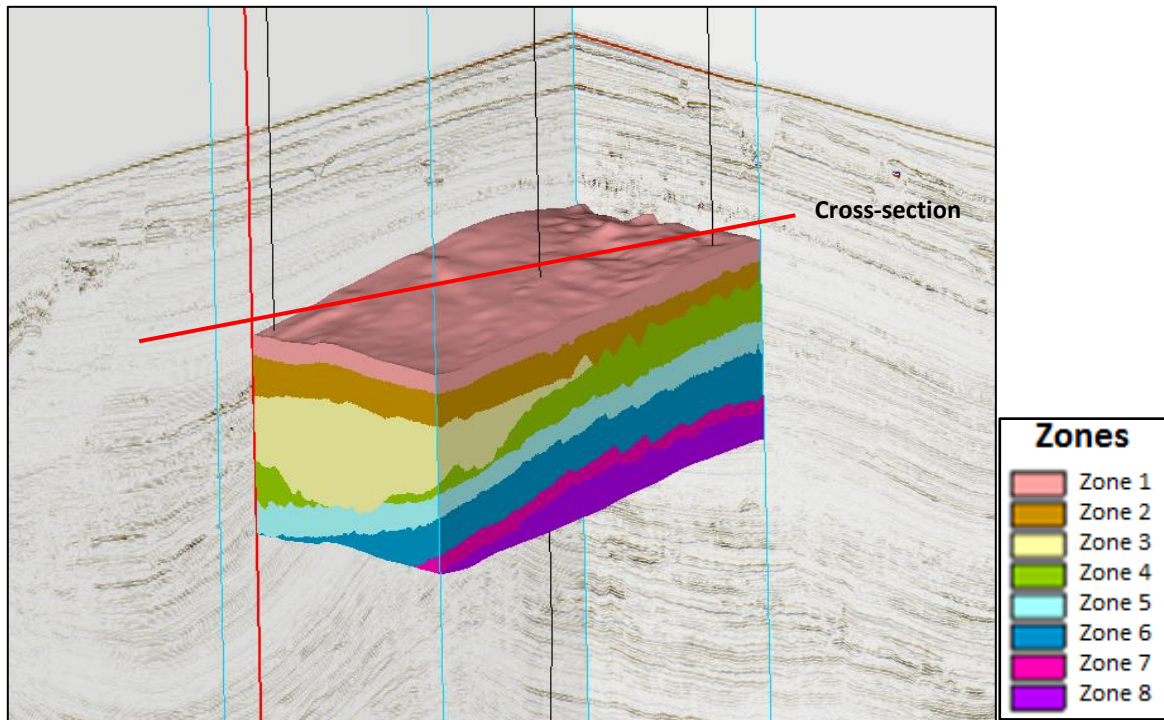


**Figure 14** - Geometrical modeling in 3D created in Petrel program with a seismic resampling within the seismic grid to obtain the elastic properties by separation of zones with the location of the cross-section (red line) Figure 12.

## 4 Geostatistical seismic inversion applied to the real case study

### 4.1 Conventional Global Stochastic Inversion

#### 4.1.1 Inversion parametrization

The spatial continuity pattern of AI was inferred by modeling experimental variograms with SGeMs. The vertical variogram was computed from the upscaled well-log data and the horizontal direction from the real fullstack seismic volume. The horizontal spatial continuity pattern was estimated from the seismic due to the large distances between wells. The recorded seismic reflection data is always a smooth representation of the natural high variability of the subsurface geology. Therefore the horizontal ranges of the variogram were adjusted manually by dividing the original range of the horizontal variograms by 2. (Table1)

Table 1: Ranges of variogram in Conventional Global Stochastic Inversion

	Max	Min	Vertical
Ranges	32	27	5

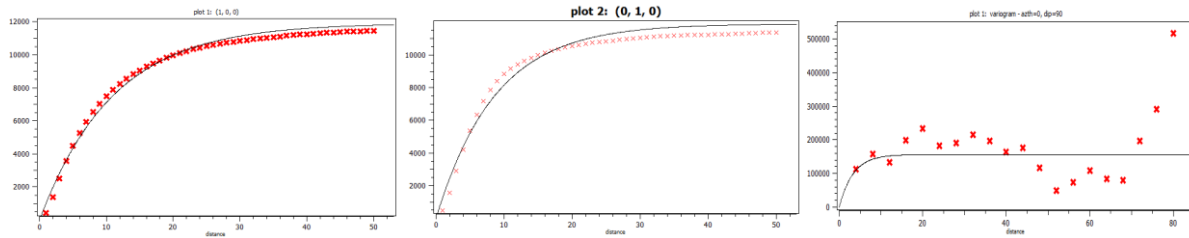


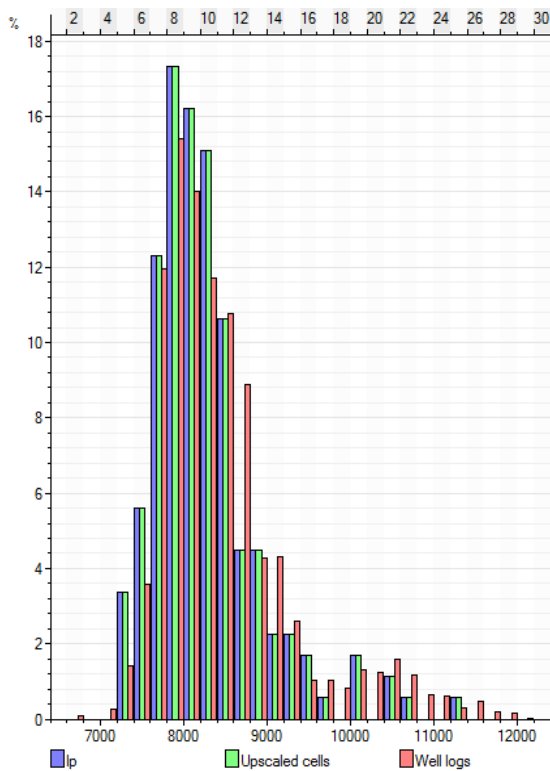
Figure 15 - Variograms, max(Left), min(center) and vertical(right). The variograms were computed using exclusively the set of conditioning well data.

Before running the iterative geostatistical seismic inversion, it was necessary to calculate the Acoustic impedance (6) from the available well-log data. Notice that the intrinsic characteristics of the prior distribution estimated from the well log, mean, variance and extreme values are preserved after the upscaling (Figure 15).

$$P \text{ impedance} = \frac{1}{DTCO} (\text{Feet/us}) \quad (4)$$

$$Vp = P \text{ impedance} * 0,3048(m) * 10^6(s) \quad (5)$$

$$\text{Acoustic impedance} = Vp * \text{Density} (kPa \cdot s/m) \quad (6)$$



Name	Min	Max	Mean	Std	Var
Property	7214.42	11213.21	8266.45	659.52	434970.4
Well logs	6611.53	12019.38	8460.36	835.2	697563

**Figure 16** - Acoustic impedance values from wells, the intrinsic characteristic of the prior distribution estimated from the well log, mean variance and extreme values are preserved after the upscaling.

#### 4.1.2 Result

The dataset described in the previous section was successfully inverted with the conventional geostatistical seismic GSI inversion algorithm (Section 2.1). The inversion methodology converged after six iterations, at each iteration, a set of 32 acoustic model of  $I_p$ , were generated recurring to DSS geostatistical sequential simulation (Soares 2001).

All individual simulations obtained at the final iteration of the iterative procedure generated synthetic seismic highly correlated with the recorded seismic reflection data. We can assess the results of this methodology by interpreting the best-fit inverse model and the mean model from the ensemble of acoustic models generated during the last iteration.

The mean model is calculated with an arithmetic mean taken the 32 simulations on a pixel-by-pixel approach. This model represents the most probable features present within the set of inverted models. Note that all the models resulting from the last iteration produce synthetic seismic very well correlated with the real one. In this case study, the resulting mean model is able to reproduce both the small and large scale details as interpreted from the real acoustic model.

The Figure below shows the best-fit inverse model and the mean model of AI computed from the ensemble of acoustic models generated during the last iteration that can be used to interpret the inversion result. Notice that the convergence of the inverted acoustic models can be evaluated by the retrieved synthetic seismic reflection data (on the right **Figure 15**) that matches considerably well in both model with the real seismic (Figure 9) in terms of spatial location, amplitude content and seismic reflection continuity.

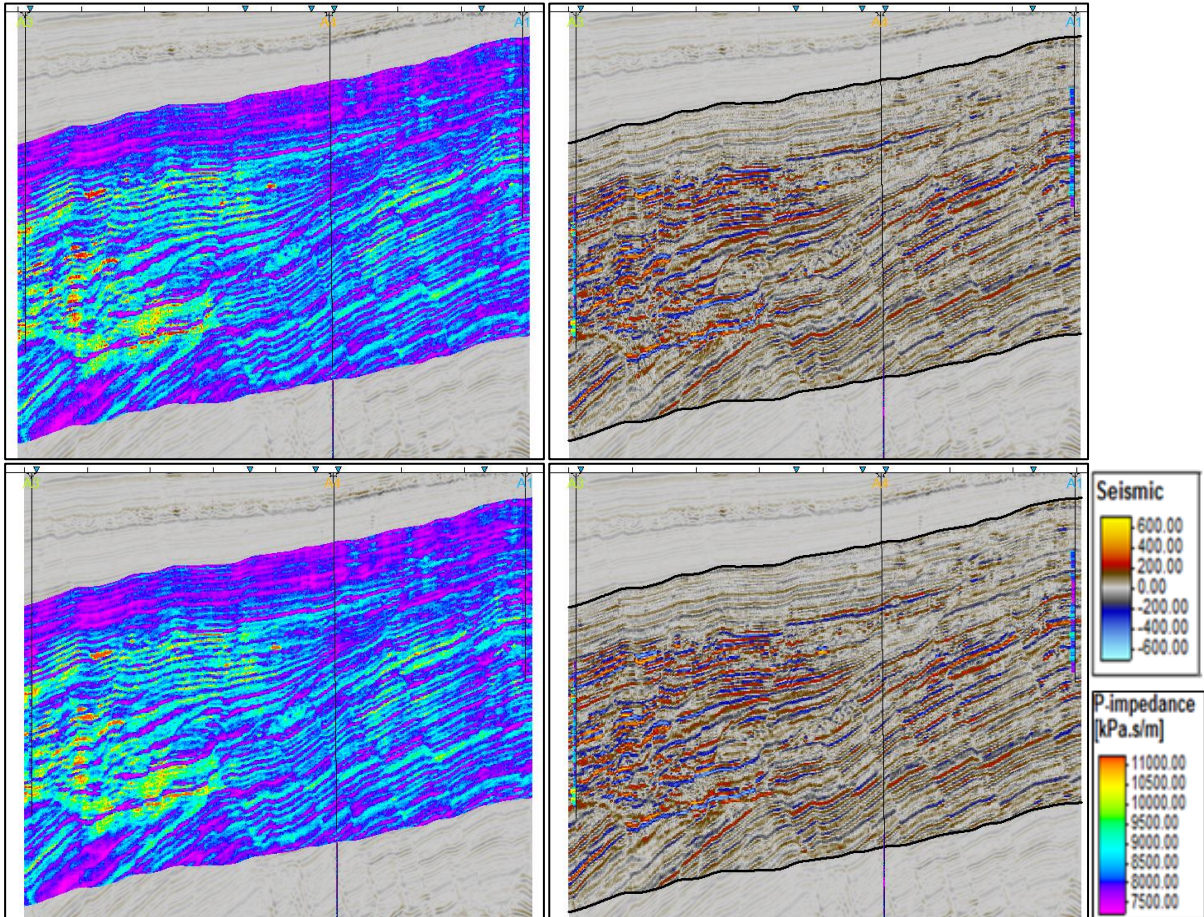


**Figure 17** - Comparison between vertical sections extracted from (on the left) acoustic model computed from the ensemble of models simulated during the last iteration and (on the right) synthetic seismic reflection data. From top to bottom: best AI model, mean AI model. For profile location see Figure 9

It is also important to highlight that the elastic inverted models from Figure 16 reproduce the spatial distribution of the original elastic properties but at the same time are able to reproduce its values and their relative variation within the areas of interest with amplitude values higher than real seismic volume. The small-scale details are extremely important for reliable reservoir characterization. All inverted models show large and small detail of interest and are constrained by the corresponding well-log data at their locations.

The synthetic seismic reflection data presents medium to high amplitude values and continuous and low acoustic impedance values as inferred from the well data present on the right in the study area close to well A1. On the left part of the section it observed discontinuity seismic reflection with different

seismic amplitudes associated with a mix between low and high amplitude values. This zone corresponds to a depositional environment with high energy.

Note that the global correlation coefficient between the recorded and the inverted seismic is more than 0.9 for both models (mean and best AI model; Figure 17).

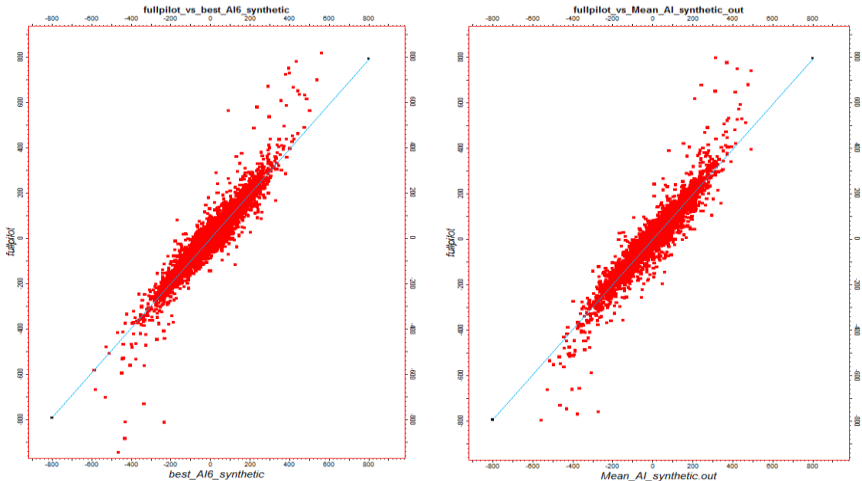


**Figure 18** - Global correlation coefficient between the recorded and the best inverted poststack seismic with a correlation of 0,951 (left) and between the recorded and the mean inverted seismic with a correlation of 0,946

The next Figure represents the local correlation coefficient volume, calculated on a trace-by-trace basis between the real seismic and the synthetic seismic volumes. The interpretation of the local correlation cubes allows the identification of those local areas where the inverted seismic did not converged and present low correlation coefficients, frequently those areas correspond to zones where the estimated wavelet is not representative of the observed seismic reflection data.

The local correlation coefficient is high for most of the trace locations. But the areas in where the synthetic seismic reflection data did not converge properly well toward the real one resulted in low local correlation coefficient, and are associated with a high degree of uncertainly.

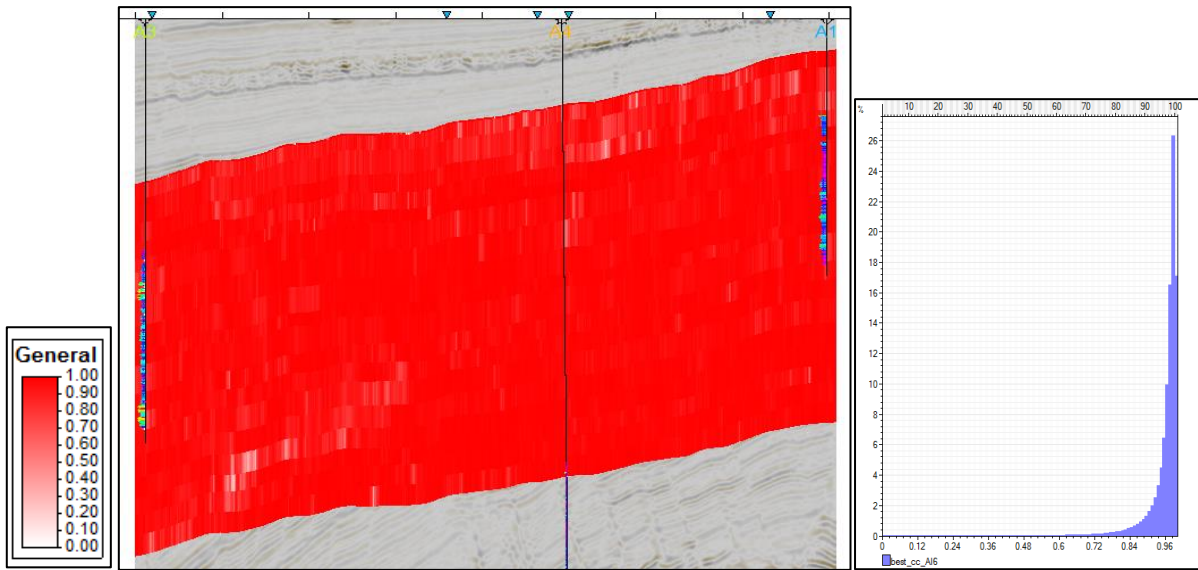


**Figure 19** - Local correlation coefficient volume calculated on a trace by trace basis between the best-fit synthetic and the real seismic volume

The spatial uncertainty of the inverted elastic property can be assessed by the interpretation of the standard deviation that represents the distribution respect to the mean or the zones with higher and lower special uncertainty. As higher is the degree of uncertainly higher will be the variability of result. In last sections the importance of this model will be discussed when both methods are compared.

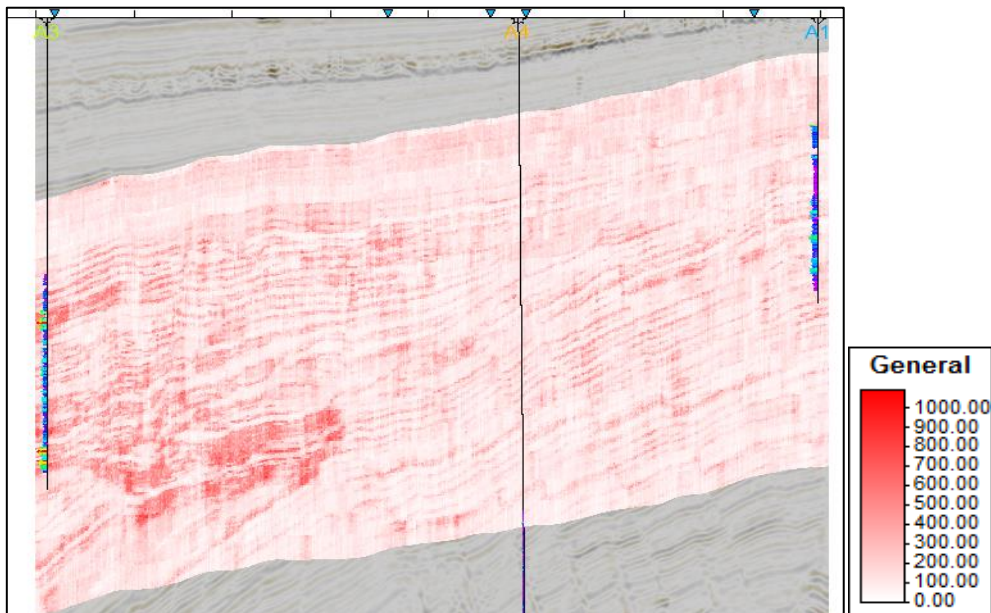


**Figure 20** - Standard deviation that represents the distribution respect to the mean.



4.1 Global Stochastic Inversion for non-stationary geological environments

4.1.1 Inversion parametrization

In the proposed methodology the simulation area is subdivided by zones (Figure 12) this zonation may be arbitrary, based on a prior knowledge of the natural system taken from seismic facies or taken into account the properties from the wells. From the experimental data obtained from each zone is defined a spatial continuity pattern given a data distribution function and a regional variogram (one for each zone).

The vertical variogram is computed from the upscaled well-log data zone-by-zone and the horizontal variograms from the real fullstack in a zone-by-zone approach as well. The horizontal spatial continuity pattern was estimated from the seismic due to the large distances between wells and the lack of data from well-log. In this case due to the lack of well data and limited data in certain zones it was imposed for each zone a variogram with the same ranges as in the traditional methodology (Table 1 and Figure 14) except for Zone 3 where continuity is very limited due to large amount of turbidite channels characteristic of the area and prevents a detailed characterization of its structure, in this case the variogram used was:

Table 2: Ranges of variogram for non-stationary geological environments

	Max	Min	Vertical
Ranges	10	10	5

For the application example with the proposed methodology due to the lack of well-log data in each zone individually, in this case, in the zones 1 and 7 (Figure 20), it was introduced the entire original distribution of acoustic impedance as conditioning distribution (Figure 15). Moreover in the zones 6 and 8 there are some experimental data but not enough samples to infer a distribution used to simulate. Therefore, the distribution as inferred from the entire dataset of acoustic impedance was used. For areas where there was few experimental data (zones 6 and 8) the global distribution of acoustic impedance was considered.

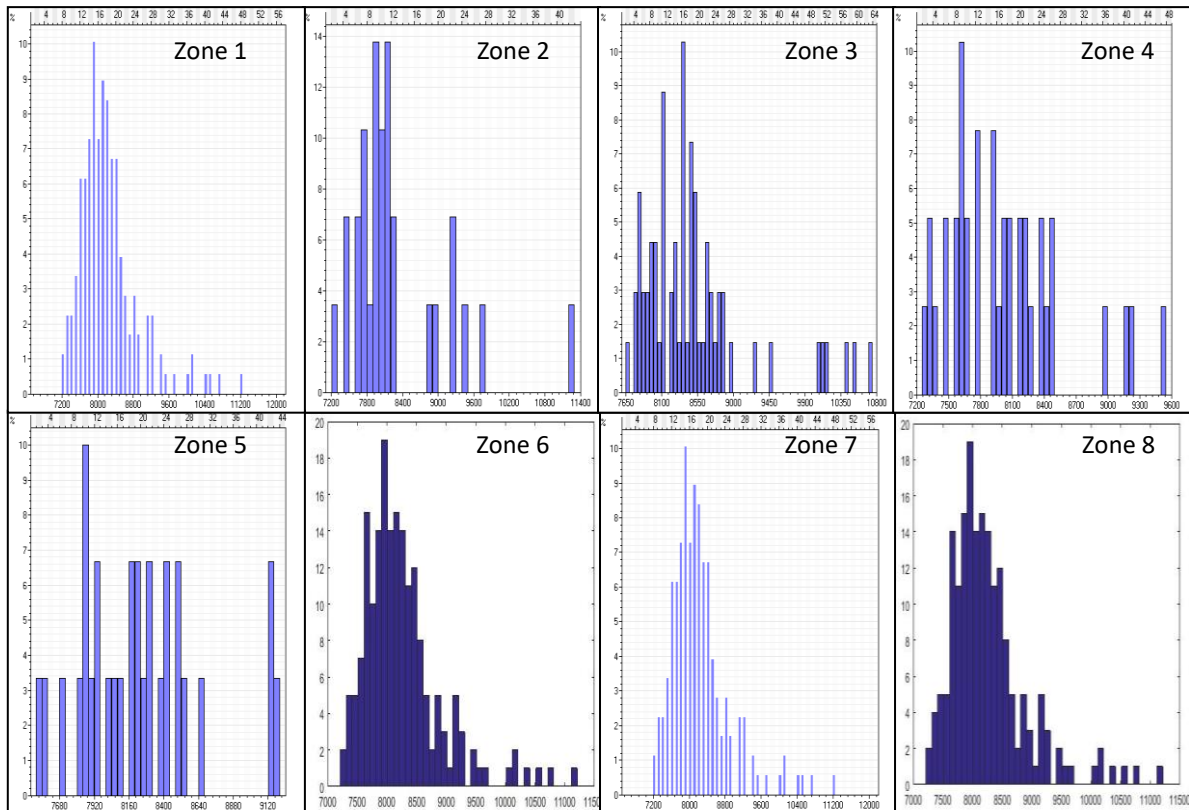


Figure 21 - Histograms of Ip dataset of all zones 1 to 8

In the proposed methodology there is the ability to integrate data from other well or taking as in this case the entire data values of some property to incorporate in the different zones is an advantage of the proposed methodology since the Ip values used to populate the conditioning distribution are assigned to each seismic unit individually (Azevedo et al.2016).

#### 4.1.2 Result

The iterative geostatistical seismic inversion GSI data regionalized by zones was concluded after 6 iteration where set of 32 acoustic model, were generated recurring to DSS geostatistical sequential simulation (Soares 2001).

From all individual simulations obtained at the end of the methodology, the best-fit and the mean model from the ensemble of acoustic model generated during the last iteration. The mean model is calculated with arithmetic mean taken the 32 simulations. Here again all the models resulting from the last iteration produce synthetic seismic very well correlated with the real one, notice that the synthetic seismic data resulting is a bit better conditioned in term of amplitude content compared with the traditional method, as the location of the main reflectors retrieve by both methodologies is similar. To

each zone the models shows coherent and continuous layers as interpreted from the real seismic reflection data (Figure 9).

The next models represents the best and mean model of AI computed by zones from the ensemble of acoustic models generated during the last iteration that can be used to interpret the inversion result.

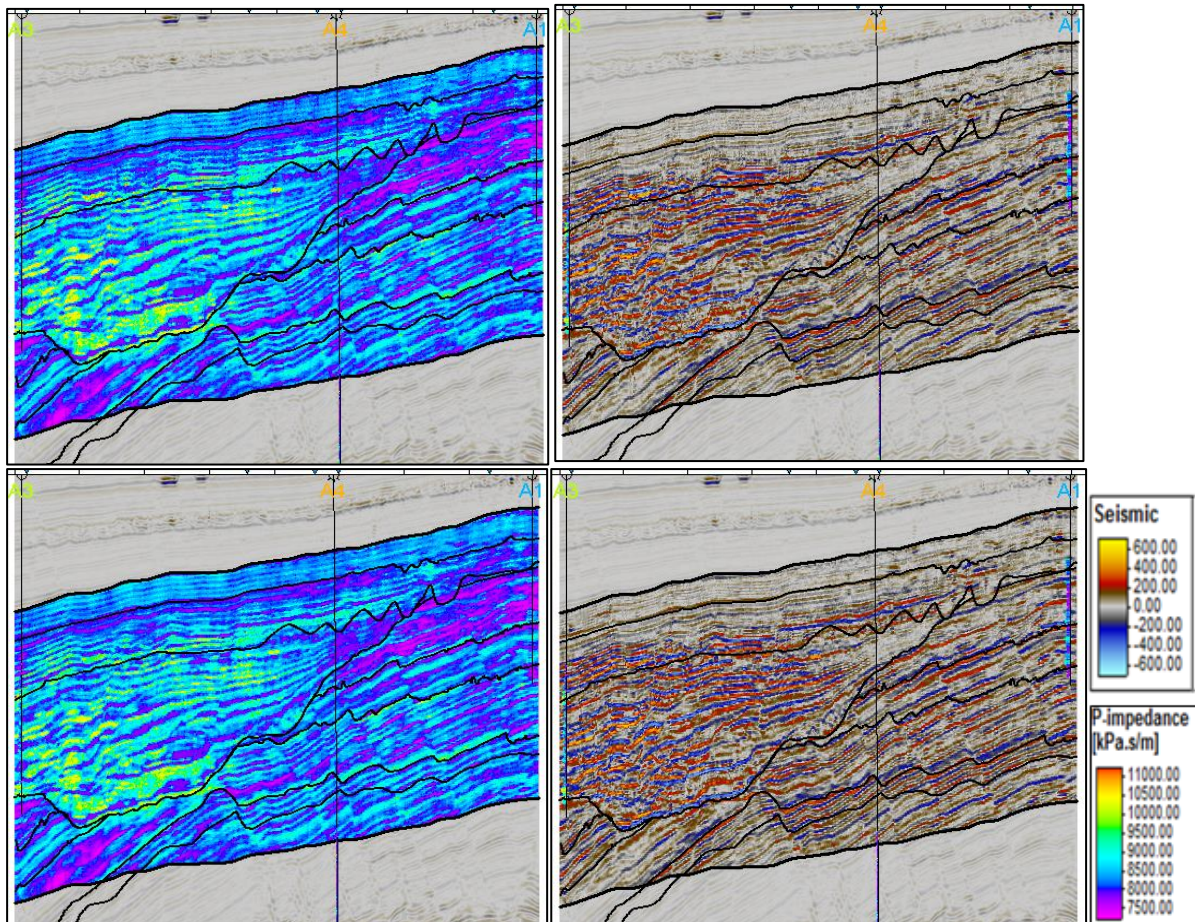


**Figure 22** - Comparison between vertical sections extracted from (on the left) acoustic model computed from the ensemble of models simulated during the last iteration and (on the right) synthetic seismic reflection data. From top to bottom: best AI model, mean AI model. For profile location see Figure 9

The synthetic seismic section computed from the best-fit inverse model and mean (on the left Figure 21) matches considerably well the real seismic (Figure 9) in term of seismic reflectors continuity, spatial location and amplitude content due to the similitude among the acoustic models generated during the last iteration.

Note that the global correlation coefficient between the recorded and the inverted poststack seismic is around 0.9 for both model (mean and best AI model). It is clear that the geostatistical seismic inversion with a regionalization model in this case is not able to reach higher global correlation coefficient between real and synthetic fullstack volume compared with the traditional GSI method (Figure 17) but enough to get reliable models of the study area.

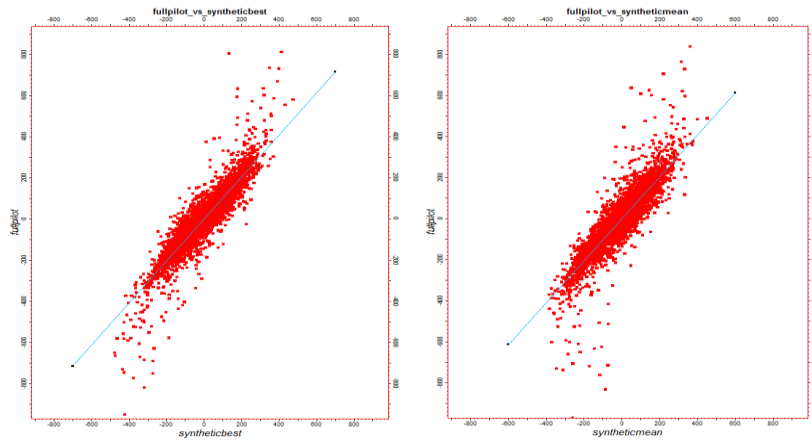


**Figure 23** - Global correlation coefficient between the recorded and the best inverted poststack seismic with a correlation of 0,91 (left) and between the recorded and the mean inverted seismic with a correlation of 0,89

Next model represent the local correlation coefficient calculated trace by trace basis between the real seismic and the synthetic seismic volumes. The local correlation coefficient is high for most of the trace locations although a little bit lower that the traditional method without zones.

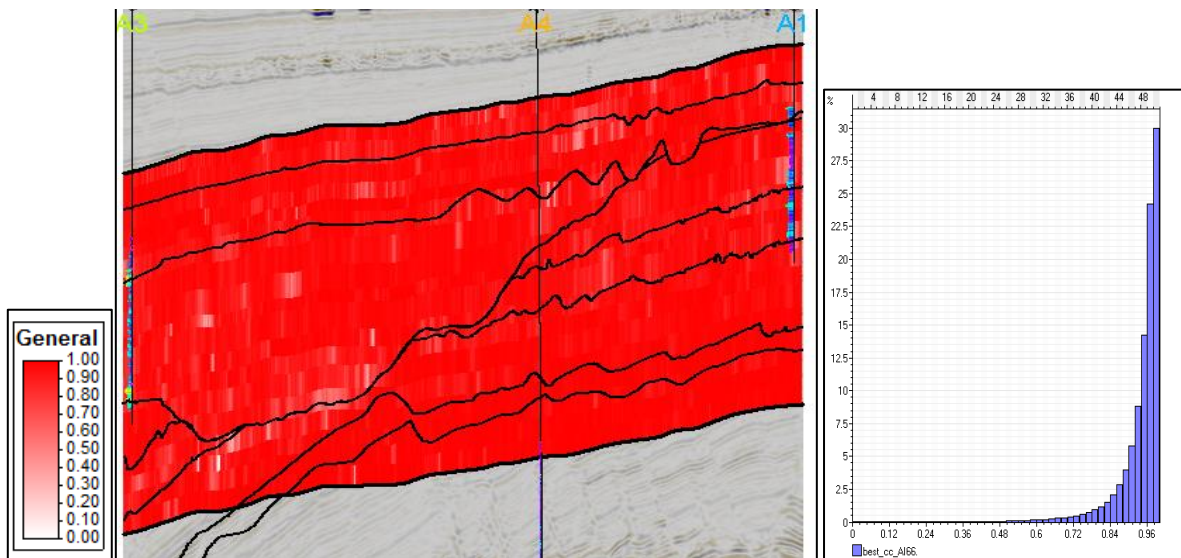


**Figure 24** - Local correlation coefficient volume of the proposed methodology by zones calculated on a trace by trace basis between the best-fit synthetic and the real seismic volume

As in another method the convergence of the inverse methodology can also be assessed by the interpretation of the standard deviation that represents the distribution respect to the mean or the zones with higher and lower special uncertainly. In last sections the importance of this model will be discussed when both methods are compared.

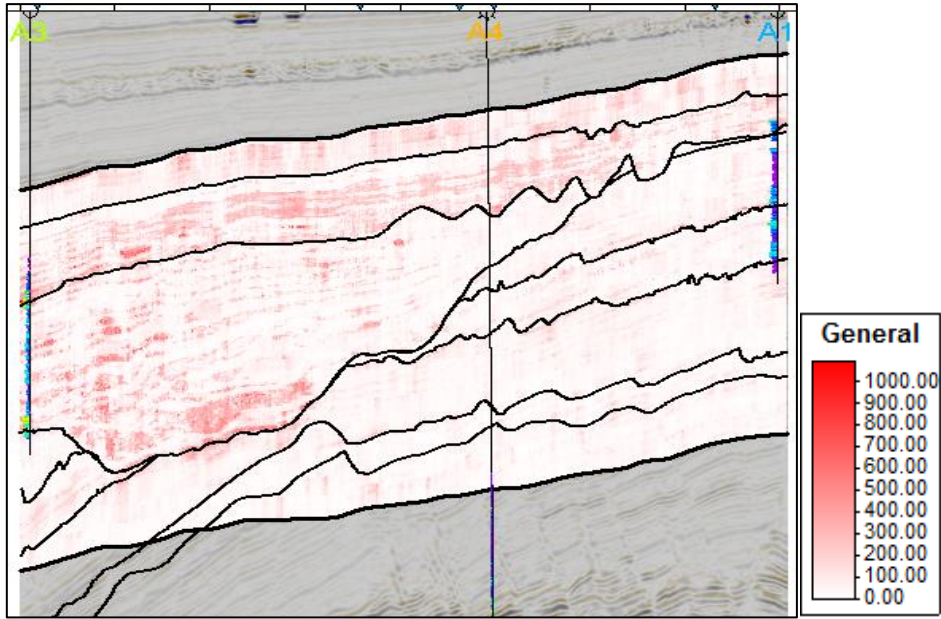


**Figure 25** - Standard deviation of the proposed methodology by zones that represent the distribution respect to the mean

## 5 Discussion

As interpreted from the available well-log data the best fit inverse  $I_p$  model retrieved from the proposed inversion technique by zones shows that for example in the zone 1 there are high AI values that agree better with the available seismic reflection data.

In the real seismic volume (on the top Figure 25) we cannot distinguish any geological layers, amplitude content or any structure within the first seismic unit. However, the best-fit inverse model from the traditional GSI shows low and high values of AI and a fine layering. The model resulting from the proposed methodology shows higher  $I_p$  values and more homogeneous distributions. In fact, the standard deviation model obtained for the proposed methodology (right at the bottom Figure 25) shows smaller values of standard deviation, meaning a lower spatial uncertainty.

When considering the rest of the zones, note that in the real seismic volume there is strong amplitude content and all zones present certain homogeneity and continuity. In the next case the zone 4 in the acoustic model retrieval is observed (Figure 26)

In this case the result in both methodologies is different with less degree of continuity and lower values of AI per zones in the proposed methodology. Observing the available well log data in well A1 allows distinguishing low  $I_p$  values in almost all that zone that does not match considerably well in terms of amplitude content, and does not make sense with the final model retrieval with the traditional GSI without zones for this specific area, where it is observed continuity and higher values of AI.

Interpreting the standard deviation in Figure 27 the proposed methodology by zones achieves a lower variance, this means that the model is closer to the real seismic volume and therefore reaches the final target of this methodology since the methodology generates models as close as possible in zones where the real seismic volume is good and therefore with lower degree of standard deviation.

Besides notice that due to the separation in the distribution of  $I_p$  values for each area there are not unreliable discontinuities between zones within the simulated models generated by the proposed methodology. The method is very flexible, allowing complex spatial regionalization to be reproduced and simple enough to use and allow high numbers of scenarios to be tested.

With the use of the traditional GSI (Soares 2007) it is get one solution with low degree of uncertainty but with the proposed methodology allow better uncertainty characterization.

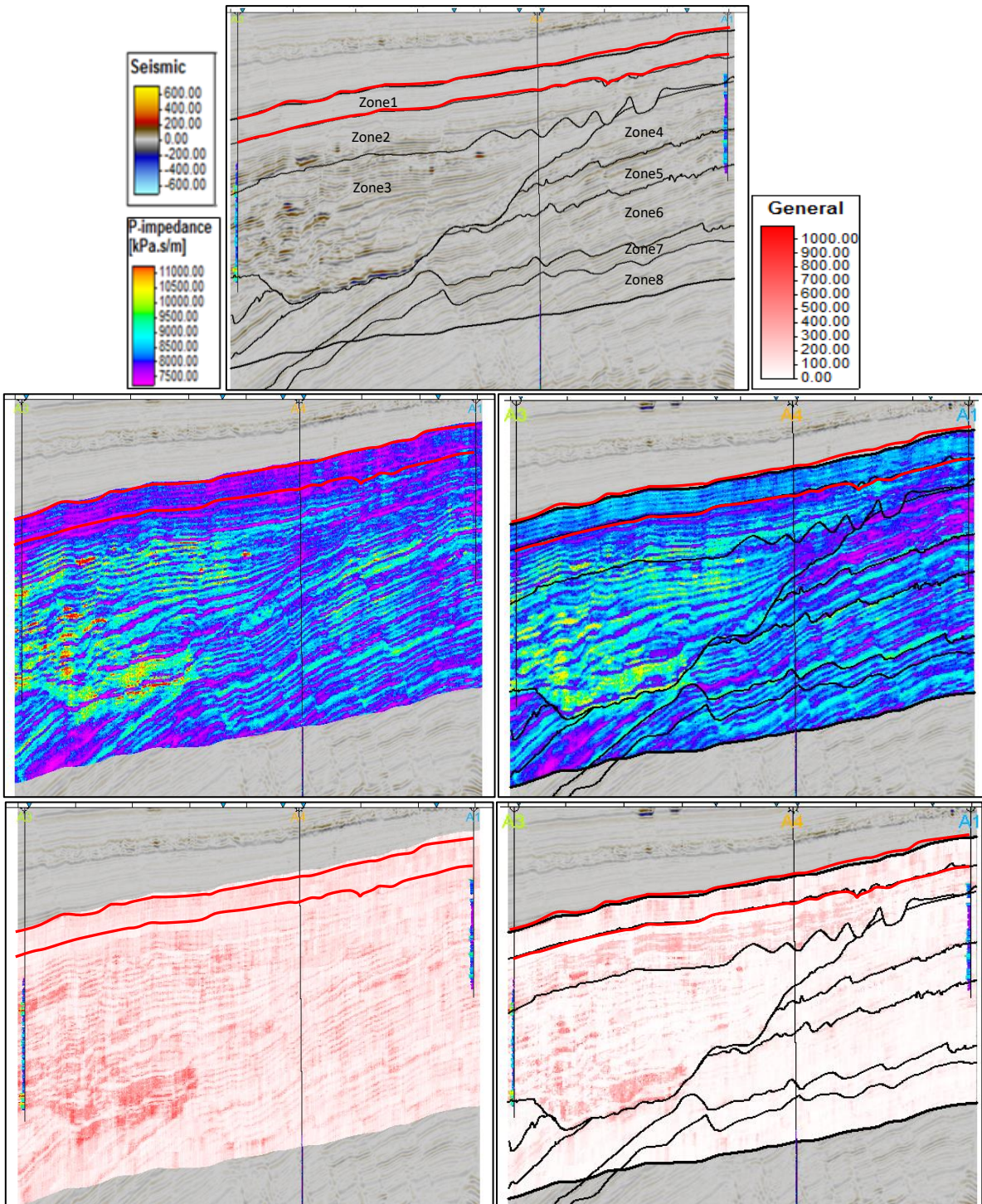


**Figure 26** – Real seismic volume (on the top) and comparison between the results obtained for zone 1 in the traditional GSI with the best seismic model and standard deviation (left) and the results obtained with the methodology proposed by zones with the best seismic model and the standard deviation (right)

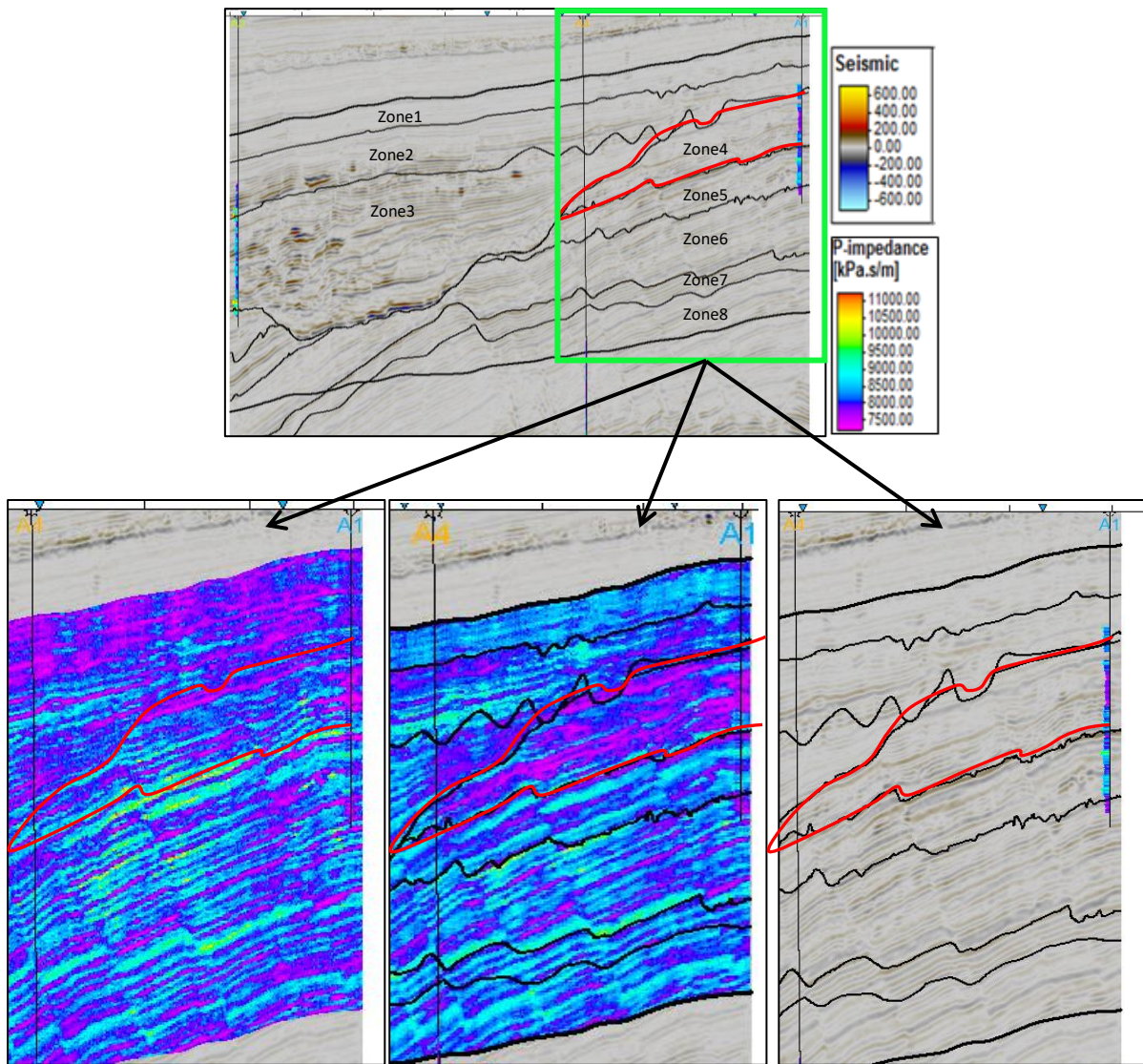


**Figure 27** - Real seismic volume (on the top) and more in detail (above right) and comparison between the results obtained for zone 4 in the traditional GSI with the best seismic model(left) and the results obtained with the methodology proposed by zones with the best seismic model(center).



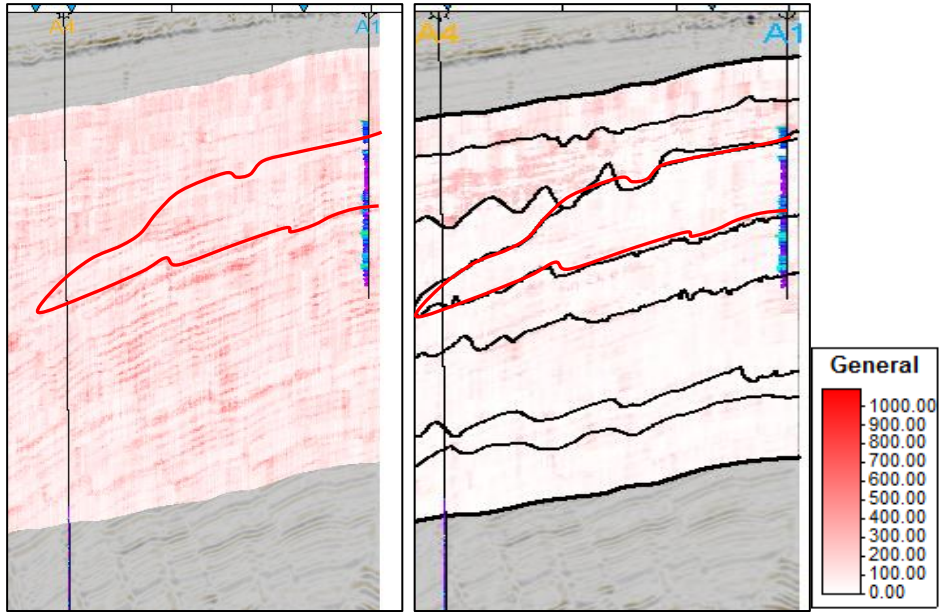


**Figure 28** - Standard deviation of the traditional GSI result (left) and of the proposed methodology by zones (right) that represent the distribution respect to the mean.

## 6 Conclusion

As conclusion the proposed technique was successfully applied to evaluate the implementation of multi-local distribution function to a real case study within a geostatistical framework. The acoustic model was computed over the entire ensemble of simulated AI models resulting from the dataset. The result showed that the retrieve inverse impedance model are able to reproduce synthetic seismic reflection data more correlated with the observed one and the synthetic volume have better amplitude content when compared with the real seismic and model are reliable and converged toward the global solution real AI model.

Also the integration of the proposed technique by zones within the inversion procedure allows that the constrained distribution function may be populated with nearby data or as in this case the total dataset in concordance with the expected geology. The proposed methodology of stochastic sequential simulation by zones has the benefit of smoothing the zone transition between zones preventing the creation of discontinuities.

Besides, the proposed technique may also be used within other different seismic inversion algorithms in order to improve the uncertainly characterization and flexibility allowing complex spatial regionalization and more number of scenarios to be tested as the AVO methodology (Azevedo. 2013) base in a global iterative geostatistical inverse procedure that allow the inversion of pre-stack seismic, sorted by angle gathers, simultaneously for density, P-wave and S-wave velocities and facies model.

In this case the facies model is part of the inverse solution obtained from available well-log and pre-stack seismic data and not derived afterward from the best-fit acoustic model, using a Bayesian classification (Avseth et al,2005) from simulated and co-simulated acoustic model of the density, as well as  $V_p/V_s$  ratio.

By changing the AVO methodology by the proposed stochastic sequential simulation methodology as the model perturbation technique of the novel approach, it will be able to integrate within the inversion procedure the regionalization model and facies definition based on the simultaneous interpretation of seismic and well-log data and geological constrains from a priori knowledge. Each zone will be constrained by a given distribution function and his corresponding spatial continuity patterns as inferred from the experimental data.

At the end the retrieved inverse models should be more geologically realistic, since they will incorporate more knowledge of the subsurface geology.

## 7 References

- Avseth,P, Mukerji.T, and Mavko.G. 2005. Quantitative Seismic Interpretation. Cambridge University Press
- Azevedo,L. 2013. "Geostatistical methods for integrating seismic reflection data into subsurface Earth models". PhD Thesis in Earth resource, Instituto Superior Técnico, Universidade de Lisboa
- Azevedo,L.,Nunes.R, Soares.A, Mundin.C, and Neto.G. 2015. Integration of well data into geostatistical seismic amplitude variation with angle inversion for facies estimation: Geophysic,80,no 6. Doi: 10.1190/GEO2015-0104.1, M113-128
- Barclay.F, Bruun.A, Camara.J, Cooke.A, Cooke.D, Gonzalez.F, 2008..."Inversion sísmica: Lectura entre líneas" Publication Schlumberger, Oilfield Review Summer. vol 20, issue 1.
- Caetano.H, 2009. "Integration of Seismic Information in Reservoir Models: Global Stochastic Inversion". PhD Thesis in Engineering sciences Instituto Superior Técnico/Universidad de Lisboa.
- Brownfield.M, Ronald.R. 2006: Geology and Total Petroleum Systems of the West-Central Coastal Province (7203), West Africa, U.S.G.S Bulletin 2207-B.
- Azevedo.L, Nunes.R, Soares.A, and Pereira.P, 2006: Geostatistical seismic inversion with direct sequential simulation and co-simulation with multi-local distribution functions, CERENA.
- Schoellkopf, N. B., and Patterson.B. A, 2000, Petroleum systems of offshore, Cabinda, Angola, in M. R. Mello and B. J. Katz, eds., Petroleum systems of South Atlantic margins: AAPG Memoir 73, p. 361–376
- Soares,A. 2006. Geoestadística para las Ciencias de la Tierra y del Ambiente, 1ª Edição. Lisboa: IST Press.
- Soares,A. 2001. "Direct sequential Simulation and Cosimulation." Mathematical Geology 33(8): 911-926
- Soares.A, Diet.JD, and Guerreiro.L. 2007. "Stochastic Inversion with a Global Perturbation Method." Petroleum Geostistics, EAGE, Cascais, Portugal (September 2007): 10-14.